Engineering Analysis with Boundary Elements ▮ (▮▮▮▮) ▮▮▮–▮▮▮

Contents lists available at ScienceDirect

Engineering Analysis with Boundary Elements

journal homepage: www.elsevier.com/locate/enganabound

# Models of corner and crack singularity of linear elastostatics and their numerical solutions

Zi-Cai Li [a,b,c], Po-Chun Chu [a,b,c], Lih-Jier Young [c,*], Ming-Gong Lee [c]

[a] Department of Applied Mathematics, National Sun Yat-sen University, Kaohsiung 80424, Taiwan
[b] Department of Computer Science and Engineering, National Sun Yat-sen University, Kaohsiung 80424, Taiwan
[c] Department of Applied Mathematics, Chung Hua University, Hsin-Chu, Taiwan

ARTICLE INFO

*Article history:*
Received 1 November 2009
Accepted 3 December 2009

*Keywords:*
Elastostatics
Corner singularity
Crack singularity
Crack tip
Crack models
Singular particular solutions
Trefftz method
Collocation Trefftz method

ABSTRACT

The singular solutions for linear elastostatics at corners are *essential* in both theory and computation. In this paper we seek the singular solutions for corners with the clamped and the free stress boundary conditions, and explore corner singularity in detail. In this paper the singular solutions of linear elastostatics are derived, and two new models of interior crack singularity are proposed. The collocation Trefftz methods are used to obtain highly accurate solutions, where the leading coefficient has 14 (or 12) significant digits by the computation with double precision. Such solutions are useful to examine other numerical methods for singularity problems in linear elastostatics. Also the explicit singular solutions can be adapted to design and develop efficient numerical methods for singularity problems, such as the combined method (Li, 1998, 2008 [19,20]) and the Trefftz methods which include the boundary approximation method (Li, 1990, Li et al., 1987 [18,26]), the collocation Trefftz method (Li et al., 2008 [24]), the hybrid Trefftz method (Qin, 2000 [36]), the boundary collocation techniques (Kolodziej and Zielinski, 2009 [16]), etc. This paper also explores a systematic analysis for singularity properties and explicit singular solutions for corners of linear elastostatics.



## 1. Introduction

The traditional finite element method (FEM) and finite difference method (FDM) provide poor accuracy of numerical solutions for singularity problems. Many innovative methods have been developed, to seek the numerical solutions with optimal convergence rates and good stability. For Poisson's equation and other elliptic equations, a systematic study is provided in Li [19]. The singular properties and the singular solutions near the corners are crucial to design effective numerical methods. Moreover, highly accurate solutions are important to examine different numerical methods. For Laplace's equation, Motz's problem is a benchmark of singularity problems, and its highly accurate solutions are provided in [19,23,26,30] by the collocation Trefftz method (CTM).

For biharmonic equation, similar models to Motz's problem are first developed in [23], and stability analysis is explored in [25]. The singular solutions near corners under free stress boundary conditions were first given in Williams [38], and then in Lin and Tong [28], Jirousek and Venkstesh [14], Jirousek and Wroblewski [15], Piltner [32], Drombosky et al. [8], and Qin [36]. In this paper, our efforts are paid to linear elastostatics, and to derive new particular solutions of linear elastostatics near corners under the clamped, and the free stress boundary conditions, in addition two new crack models are proposed. It is worthy pointing out that the singular solutions near corners in this paper directly from free stress boundary conditions are coincident with those in [38,28] from biharmonic equations by using a similarity mapping.

The singular properties and the explicit singular solutions of linear elastostatics at corners are *essential* in both theory and computation. Once the singularity of corner solutions is known, the reduced convergence rates of FEM, FDM, FVM and other numerical methods are found (see Section 7.2), and some improved techniques can be invented, to recover the optimal convergence rates (see [19]). Moreover, once the explicit singular solutions are known, some models as in Sections 4 and 6 can be designed, and the collocation Trefftz method can be used to give their highly accurate solutions, which can be used for testing other numerical methods (also see [19]). More importantly, based on the explicit particular solutions of corners given in this paper, we may develop a number of efficient numerical methods for linear elastostatics, such as the Trefftz methods including the collocation Trefftz method and the hybrid Trefftz method, and the combinations (see [1,4,7–9,12,17,20,27,29,34,35,39].)

This paper is organized as follows. In Section 2, a basic description for elastostatics problems in 2D is introduced, and their particular solutions are provided. In Section 3, singular

* Corresponding author.
*E-mail addresses:* zcli@math.nsysu.edu.tw (Z.-C. Li), young@chu.edu.tw (L.-J. Young).

0955-7997/$ - see front matter © 2010 Elsevier Ltd. All rights reserved.
doi:10.1016/j.enganabound.2010.01.001

solutions near corners are derived for the clamped boundary conditions. In Section 4, a model of crack singularity with clamped boundary conditions is designed, and its numerical solutions are sought by the collocation Trefftz method (CTM) as in [19,24]. In Section 5, singular solutions near corners are derived for the free stress boundary conditions, and in Section 6 the other model of crack singularity with free stress is designed, and numerical results are also provided. In Section 7, the algorithms are given for the leading powers $v_k$ of the corner solution $O(r^{v_k})$, and numerical results are provided for the rectangular corner and the concave corner of the L-shaped domain. In the last section, a few concluding remarks are made.

## 2. Linear elastostatics problems in 2D

### 2.1. Basic equations

Consider the linear elastostatics problem in 2D. Denote the displacement vector,

$$\vec{w}=\mathbf{w}=\{w_1(\mathbf{x}),w_2(\mathbf{x})\}^T=\{u(x,y),v(x,y)\}^T, \tag{2.1}$$

where $\vec{x}=\mathbf{x}=(x_1,x_2)=(x,y)$. The linear strain tensor is given by

$$\varepsilon_{ij}(\mathbf{x})=\frac{1}{2}\left[\frac{\partial w_i(\mathbf{x})}{\partial x_j}+\frac{\partial w_j(\mathbf{x})}{\partial x_i}\right],\quad 1\le i,j\le 2. \tag{2.2}$$

Let $\sigma_{ij}$ $(1\le i,j\le 2)$ denote the stress tensor at $\mathbf{x}$. For an isotropic homogeneous Hookean solid, there exist the stress–strain relations

$$\sigma_{ij}=\lambda(\nabla\cdot\vec{w})\delta_{ij}+2\mu\varepsilon_{ij},\quad 1\le i,j\le 2, \tag{2.3}$$

where " $\nabla\cdot$ " is the divergence operator, $\lambda$ and $\mu$ are the Lamé constants, and $\delta_{ij}$ is the Kronecker delta.

When there exists a body force $\vec{f}$, we obtain the nonhomogeneous equation, called the Lamé system for isotropic body:

$$\mu\Delta\vec{w}+(\lambda+\mu)\nabla(\nabla\cdot\vec{w})+\vec{f}=0\quad\text{in } S. \tag{2.4}$$

When $\vec{f}\equiv\vec{0}$, we have the Cauchy–Navier equation of linear elastostatics:

$$\Delta\vec{w}+\frac{1}{1-2v}\nabla(\nabla\cdot\vec{w})=0\quad\text{in } S, \tag{2.5}$$

where the Poisson ratio

$$v=\frac{\lambda}{2(\lambda+\mu)},\quad 0<v<\frac{1}{2}. \tag{2.6}$$

Young's modulus $E$ and the bulk modulus $K$ are introduced by

$$E=\frac{\mu(3\lambda+2\mu)}{\lambda+\mu},\quad K=\frac{E}{3(1-2v)}. \tag{2.7}$$

The inverse relations of (2.6) and (2.7) are given by

$$\lambda=\frac{Ev}{(1+v)(1-2v)},\quad \mu=\frac{E}{2(1+v)}. \tag{2.8}$$

The strain–stress relations are given by

$$\varepsilon_{ij}=\frac{1+v}{E}\sigma_{ij}-\frac{v}{E}\delta_{ij}\sum_{k=1}^{2}\sigma_{kk}. \tag{2.9}$$

There also exist the symmetric relations:

$$\sigma_{ij}=\sigma_{ji},\quad \varepsilon_{ij}=\varepsilon_{ji}. \tag{2.10}$$

Denote the constant

$$\kappa=\frac{1}{4(1-v)}. \tag{2.11}$$

For the plane strain problem the constant is given by

$$D=\frac{\lambda+\mu}{\lambda+3\mu}=\frac{1}{3-4v}=\frac{\kappa}{1-\kappa}, \tag{2.12}$$

and for the plane stress problem,

$$D=\frac{1}{3-4v}=\frac{1+\hat{v}}{3-\hat{v}},\quad v=\frac{\hat{v}}{1+\hat{v}}. \tag{2.13}$$

.

### 2.2. Traction boundary conditions

The Cauchy–Navier equation (2.5) is written explicitly by

$$\mu\Delta u+(\lambda+\mu)\left\{\frac{\partial^2 u}{\partial x^2}+\frac{\partial^2 v}{\partial x\partial y}\right\}=0\quad\text{in } S, \tag{2.14}$$

$$\mu\Delta v+(\lambda+\mu)\left\{\frac{\partial^2 u}{\partial x\partial y}+\frac{\partial^2 v}{\partial y^2}\right\}=0\quad\text{in } S, \tag{2.15}$$

or by

$$\Delta u+\frac{1}{1-2v}\left\{\frac{\partial^2 u}{\partial x^2}+\frac{\partial^2 v}{\partial x\partial y}\right\}=0\quad\text{in } S, \tag{2.16}$$

$$\Delta v+\frac{1}{1-2v}\left\{\frac{\partial^2 u}{\partial x\partial y}+\frac{\partial^2 v}{\partial y^2}\right\}=0\quad\text{in } S, \tag{2.17}$$

where $v$ is given in (2.6). The traction on $\partial S$ is given by

$$\vec{\tau}(\vec{w})(\mathbf{x})=(\tau_1(u,v),\tau_2(u,v))^T, \tag{2.18}$$

where the components

$$\tau_1(u,v)=\sigma_x n_1+\sigma_{xy}n_2=\lambda\left(\frac{\partial u}{\partial x}+\frac{\partial v}{\partial y}\right)n_1+2\mu\frac{\partial u}{\partial v}+\mu n_2\left(\frac{\partial v}{\partial x}-\frac{\partial u}{\partial y}\right), \tag{2.19}$$

$$\tau_2(u,v)=\sigma_{xy}n_1+\sigma_y n_2=\lambda\left(\frac{\partial u}{\partial x}+\frac{\partial v}{\partial y}\right)n_2+2\mu\frac{\partial v}{\partial v}-\mu n_1\left(\frac{\partial v}{\partial x}-\frac{\partial u}{\partial y}\right), \tag{2.20}$$

where $n_1=\cos(v,x)$, $n_2=\cos(v,y)$, and the stress

$$\sigma_x=\sigma_{11},\quad \sigma_y=\sigma_{22},\quad \sigma_{xy}=\sigma_{12}=\sigma_{21}. \tag{2.21}$$

### 2.3. Particular solutions

In Jirousek and Wroblewski [15], Jirousek and Venkstesh [14] and Qin [36], for the plane stress equations (2.16) and (2.17), the particular solutions are expressed as the complex functions. Denote $i=\sqrt{-1}$, $\mathbf{z}=x+iy=re^{i\theta}$, $\overline{\mathbf{z}}=x-iy=re^{-i\theta}$. The particular solutions $u(x,y)$ and $v(x,y)$ of the plane stress equations are given by the real and imaginary parts of $A_k, B_k, C_k$ and $D_k$ below, respectively,

$$A_k=i\mathbf{z}^k+iDk\mathbf{z}\overline{\mathbf{z}}^{k-1}, \tag{2.22}$$

$$B_k=\mathbf{z}^k-Dk\mathbf{z}\overline{\mathbf{z}}^{k-1}, \tag{2.23}$$

$$C_k=i\overline{\mathbf{z}}^k, \tag{2.24}$$

$$D_k=-\overline{\mathbf{z}}^k,\quad k=1,2\ldots, \tag{2.25}$$

where $D$ is given in (2.12) or (2.13). We have the following linear combination for the Trefftz method (TM):

$$u_L=\sum_{k=1}^{L}\{a_k\Re(A_k)+b_k\Re(B_k)+c_k\Re(C_k)+d_k\Re(D_k)\}+d_0, \tag{2.26}$$

$$v_L=\sum_{k=1}^{L}\{a_k\Im(A_k)+b_k\Im(B_k)+c_k\Im(C_k)+d_k\Im(D_k)\}+c_0, \tag{2.27}$$

Please cite this article as: Li Z-C, et al. Models of corner and crack singularity of linear elastostatics and their numerical solutions. Eng Anal Bound Elem (2010), doi:10.1016/j.enganabound.2010.01.001

where $a_k, b_k, c_k, d_k, c_0$ and $d_0$ are the constants, and the notations $\Re$ and $\Im$ are the real and the imaginary parts, respectively. In (2.26) and (2.27) $u=\Re(A_1)=-(1+D)y$ and $v=\Im(A_1)=(1+D)x$ denote a rigid motion.

From (2.26) and (2.27) we have the complete particular solutions (also see [15,36]),

$$u_L=\sum_{k=1}^{L} r^k\{a_k[-\sin k\theta+Dk\sin(k-2)\theta]+b_k[\cos k\theta-Dk\cos(k-2)\theta] +c_k\sin k\theta-d_k\cos k\theta\}+d_0, \tag{2.28}$$

$$v_L=\sum_{k=1}^{L} r^k\{a_k[\cos k\theta+Dk\cos(k-2)\theta]+b_k[\sin k\theta+Dk\sin(k-2)\theta] +c_k\cos k\theta+d_k\sin k\theta\}+c_0. \tag{2.29}$$

## 3. Singular solutions near corners under clamped boundary conditions

Choose the sectorial domain $S=\{(r,\theta)|(0\le R,-\Theta\le\theta\le\Theta)\}$, where $\Theta\in(0,\pi]$. First consider the displacement conditions at two edges of corner $O$ with the clamped boundary conditions

$$u=v=0 \quad \text{on } \theta=\pm\Theta. \tag{3.1}$$

The singularity solutions can be obtained from (2.22) to (2.25) by replacing the integer $k$ with a complex number $v^*=v_k=\alpha_k+i\beta_k$,[1] where $\alpha_k$ and $\beta_k$ are real and $i=\sqrt{-1}$. Then the general singular solutions are given from (2.28) and (2.29)

$$u_L=\sum_{k=1}^{L} r^{v_k}\{a_k[-\sin v_k\theta+Dv_k\sin(v_k-2)\theta]+b_k[\cos v_k\theta -Dv_k\cos(v_k-2)\theta]+c_k\sin v_k\theta-d_k\cos v_k\theta\}+d_0, \tag{3.2}$$

$$v_L=\sum_{k=1}^{L} r^{v_k}\{a_k[\cos v_k\theta+Dv_k\cos(v_k-2)\theta]+b_k[\sin v_k\theta +Dv_k\sin(v_k-2)\theta]+c_k\cos v_k\theta+d_k\sin v_k\theta\}+c_0, \tag{3.3}$$

where $a_k, b_k, c_k$ and $d_k$ are real coefficients, and $D$ is given in (2.12) or (2.13). In (3.2) and (3.3), we choose a group of four coefficients $a_k, b_k, c_k$ and $d_k$ to satisfy the boundary conditions in (3.1), to obtain $d_0=c_0=0$ and the matrix equation

$$\mathbf{By}=\mathbf{0}, \tag{3.4}$$

where $\mathbf{y}=(a,b,c,d)^T$ and the matrix is given by

$$\mathbf{B}=\begin{pmatrix} -\sin v^*\Theta+Dv^*\sin(v^*-2)\Theta & \cos v^*\Theta-Dv^*\cos(v^*-2)\Theta & \sin v^*\Theta & -\cos v^*\Theta\\ \cos v^*\Theta+Dv^*\cos(v^*-2)\Theta & \sin v^*\Theta+Dv^*\sin(v^*-2)\Theta & \cos v^*\Theta & \sin v^*\Theta\\ \sin v^*\Theta-Dv^*\sin(v^*-2)\Theta & \cos v^*\Theta-Dv^*\cos(v^*-2)\Theta & -\sin v^*\Theta & -\cos v^*\Theta\\ \cos v^*\Theta+Dv^*\cos(v^*-2)\Theta & -\sin v^*\Theta-Dv^*\sin(v^*-2)\Theta & \cos v^*\Theta & -\sin v^*\Theta \end{pmatrix}. \tag{3.5}$$

The sufficient and necessary condition of existence of nonzero solutions $\mathbf{y}$ is that the determinant of matrix $\mathbf{B}$ is zero,

$$\begin{vmatrix} -\sin v^*\Theta+Dv^*\sin(v^*-2)\Theta & \cos v^*\Theta-Dv^*\cos(v^*-2)\Theta & \sin v^*\Theta & -\cos v^*\Theta\\ \cos v^*\Theta+Dv^*\cos(v^*-2)\Theta & \sin v^*\Theta+Dv^*\sin(v^*-2)\Theta & \cos v^*\Theta & \sin v^*\Theta\\ \sin v^*\Theta-Dv^*\sin(v^*-2)\Theta & \cos v^*\Theta-Dv^*\cos(v^*-2)\Theta & -\sin v^*\Theta & -\cos v^*\Theta\\ \cos v^*\Theta+Dv^*\cos(v^*-2)\Theta & -\sin v^*\Theta-Dv^*\sin(v^*-2)\Theta & \cos v^*\Theta & -\sin v^*\Theta \end{vmatrix}=0. \tag{3.6}$$

We have a lemma.

[1] In this paper, the complex numbers $v^*$ and $v_k$ are used, which are different from the Poisson ratio $v$ in (2.6).

**Lemma 3.1.** *For nonzero solutions of the equations*

$$\begin{pmatrix} b_{11} & b_{12} & b_{13} & b_{14}\\ b_{21} & b_{22} & b_{23} & b_{24}\\ -b_{11} & b_{12} & -b_{13} & b_{14}\\ b_{21} & -b_{22} & b_{23} & -b_{24} \end{pmatrix}\begin{pmatrix} a\\ b\\ c\\ d \end{pmatrix}=\vec{0}, \tag{3.7}$$

*there exist the equalities*

$$\begin{vmatrix} b_{11} & b_{13}\\ b_{21} & b_{23} \end{vmatrix}=0, \quad \begin{vmatrix} b_{12} & b_{14}\\ b_{22} & b_{24} \end{vmatrix}=0. \tag{3.8}$$

**Proof.** We may split the equations in (3.7) as follows. In (3.7), by subtracting the third equation from the first equation, and by adding the second and the fourth equations, we have

$$2b_{11}a+2b_{13}c=0, \quad 2b_{21}a+2b_{23}c=0. \tag{3.9}$$

The existence of nonzero solutions of $a$ and $c$ implies

$$\begin{vmatrix} b_{11} & b_{13}\\ b_{21} & b_{23} \end{vmatrix}=0. \tag{3.10}$$

Similarly, in (3.7) by adding the first and the third equations, and by subtracting the fourth from the second equations, we have

$$2b_{12}b+2b_{14}d=0, \quad 2b_{22}b+2b_{24}d=0. \tag{3.11}$$

The existence of nonzero solutions of $b$ and $d$ implies

$$\begin{vmatrix} b_{12} & b_{14}\\ b_{22} & b_{24} \end{vmatrix}=0. \tag{3.12}$$

This completes the proof of Lemma 3.1. □

**Theorem 3.1.** *Let* (3.6) *be given for the clamped boundary conditions* (3.1). *There exist the equalities*

$$\sin 2v^*\Theta=\pm Dv^*\sin 2\Theta, \tag{3.13}$$

*where the signs " +" and " −" correspond to the symmetric and the anti-symmetric solution $u, v$, respectively.*

**Proof.** Based on Lemma 3.1, we have from (3.6)

$$\begin{vmatrix} -\sin v^*\Theta+Dv^*\sin(v^*-2)\Theta & \sin v^*\Theta\\ \cos v^*\Theta+Dv^*\cos(v^*-2)\Theta & \cos v^*\Theta \end{vmatrix}=0 \tag{3.14}$$

and

$$\begin{vmatrix} \cos v^*\Theta-Dv^*\cos(v^*-2)\Theta & -\cos v^*\Theta\\ \sin v^*\Theta+Dv^*\sin(v^*-2)\Theta & \sin v^*\Theta \end{vmatrix}=0. \tag{3.15}$$

From (3.14) there is the equality,

$$(-\sin v^*\Theta+Dv^*\sin(v^*-2)\Theta)\cos v^*\Theta =(\cos v^*\Theta+Dv^*\cos(v^*-2)\Theta)\sin v^*\Theta.$$

Since

$$\sin(v^*-2)\Theta=\sin v^*\Theta\cos 2\Theta-\cos v^*\Theta\sin 2\Theta, \tag{3.16}$$

$$\cos(v^*-2)\Theta=\cos v^*\Theta\cos 2\Theta+\sin v^*\Theta\sin 2\Theta, \tag{3.17}$$

we have

$$2\sin v^*\Theta\cos v^*\Theta=-Dv^*(\cos^2 v^*\Theta+\sin^2 v^*\Theta)\sin 2\Theta, \tag{3.18}$$

that is,

$$\sin 2v^*\Theta=-Dv^*\sin 2\Theta. \tag{3.19}$$

This is the desired result (3.13) with sign " −" .

Similarly, we have from (3.15)

$$(\cos v^*\Theta-Dv^*\cos(v^*-2)\Theta)\sin v^*\Theta=-(\sin v^*\Theta+Dv^*\sin(v^*-2)\Theta)\cos v^*\Theta.$$

From (3.16) and (3.17) we have

$$\sin 2v^*\Theta=Dv^*\sin 2\Theta. \tag{3.20}$$

Please cite this article as: Li Z-C, et al. Models of corner and crack singularity of linear elastostatics and their numerical solutions. Eng Anal Bound Elem (2010), doi:10.1016/j.enganabound.2010.01.001

Combining (3.19) and (3.20) yields the desired results (3.13) with sign " $\pm$ ".

The equality (3.13) with sign " $+$" results from (3.15), which denotes the nonzero coefficients $b_k$ and $d_k$ of symmetric solutions $u, v$ in (3.2) and (3.3) satisfying $\partial u/\partial y = v = 0$ at $\theta = 0$. Also the equality (3.13) with the sign " $-$" responds to the nonzero $a_k$ and $c_k$ of the anti-symmetric solutions $u, v$ satisfying $u = \partial v/\partial y = 0$ at $\theta = 0$. This completes the proof of Theorem 3.1. □

When the real or the complex root $v_k$ are obtained from (3.13), the coefficients satisfy the following relations:

$$c_k = p_k a_k, \quad d_k = q_k b_k, \tag{3.21}$$

where $p_k$ and $q_k$ may be complex, given by

$$p_k = -\{Dv_k \cos 2\Theta + \sqrt{1-(Dv_k \sin 2\Theta)^2}\}, \tag{3.22}$$

$$q_k = -Dv_k \cos 2\Theta + \sqrt{1-(Dv_k \sin 2\Theta)^2}. \tag{3.23}$$

Then the particular solutions of (3.2) and (3.3) are simplified as

$$\begin{aligned} u_L = \sum_{k=1}^{L} \Re\{r^{v_k}\{a_k[(-1+p_k)\sin v_k\theta + Dv_k \sin(v_k-2)\theta] \\ + b_k[(1-q_k)\cos v_k\theta - Dv_k \cos(v_k-2)\theta]\}, \end{aligned} \tag{3.24}$$

$$\begin{aligned} v_L = \sum_{k=1}^{L} \Re\{r^{v_k}\{a_k[(1+p_k)\cos v_k\theta + Dv_k \cos(v_k-2)\theta] \\ + b_k[(1+q_k)\sin v_k\theta + Dv_k \sin(v_k-2)\theta]\}, \end{aligned} \tag{3.25}$$

where $a_k$ and $b_k$ are still real.

Below, let us derive the constants $p_k$ and $q_k$ in (3.22) and (3.23). In general, we assume

$$\cos v^*\Theta \neq 0, \quad \sin v^*\Theta \neq 0. \tag{3.26}$$

Otherwise, when $\cos v^*\Theta = 0$ (i.e., $v^*\Theta = (n+\frac{1}{2})\pi$) and $\sin v^*\Theta = 0$ (i.e., $v^*\Theta = n\pi$), the coefficient relations are given in the next section. The relation between coefficients $a$ and $c$ can be found in (3.14) under (3.19)

$$c = \frac{1}{\sin v^*\Theta}(\sin v^*\Theta - Dv^* \sin(v^*-2)\Theta)a, \tag{3.27}$$

to give

$$\begin{aligned} p(v^*) &= \frac{1}{\sin v^*\Theta}(\sin v^*\Theta - Dv^* \sin(v^*-2)\Theta) \\ &= 1 - Dv^* \frac{1}{\sin v^*\Theta}(\sin v^*\Theta \cos 2\Theta - \cos v^*\Theta \sin 2\Theta) \\ &= 1 - Dv^* \cos 2\Theta + Dv^* \frac{1}{\sin v^*\Theta} \cos v^*\Theta \sin 2\Theta \\ &= 1 - Dv^* \cos 2\Theta + Dv^* \frac{1}{\sin v^*\Theta} \cos v^*\Theta \left[-\frac{\sin 2v^*\Theta}{Dv^*}\right] \\ &= 1 - Dv^* \cos 2\Theta - 2(\cos v^*\Theta)^2, \end{aligned} \tag{3.28}$$

where we have used (3.19). Since $2\cos^2 x = 1 + \cos 2x$ we have from (3.28)

$$\begin{aligned} p(v^*) &= 1 - Dv^* \cos 2\Theta - 1 - \cos 2v^*\Theta \\ &= -Dv^* \cos 2\Theta - \sqrt{1-(\sin 2v^*\Theta)^2} \\ &= -\{Dv^* \cos 2\Theta + \sqrt{1-(Dv^* \sin 2\Theta)^2}\}. \end{aligned} \tag{3.29}$$

This is the first desired result (3.22) with $v^* = v_k$.

Next for coefficients $b$ and $d$, we have from (3.15) under (3.20),

$$d = \frac{1}{\cos v^*\Theta}(\cos v^*\Theta - Dv^* \cos(v^*-2)\Theta)b = q(v^*)b, \tag{3.30}$$

to give

$$\begin{aligned} q(v^*) &= \frac{1}{\cos v^*\Theta}(\cos v^*\Theta - Dv^* \cos(v^*-2)\Theta) \\ &= 1 - Dv^* \frac{1}{\cos v^*\Theta}(\cos v^*\Theta \cos 2\Theta + \sin v^*\Theta \sin 2\Theta) \\ &= 1 - Dv^* \cos 2\Theta - Dv^* \frac{1}{\cos v^*\Theta} \sin v^*\Theta \sin 2\Theta \\ &= 1 - Dv^* \cos 2\Theta - Dv^* \frac{1}{\cos v^*\Theta} \sin v^*\Theta \left[\frac{\sin 2v^*\Theta}{Dv^*}\right] \\ &= 1 - Dv^* \cos 2\Theta - 2(\sin v^*\Theta)^2. \end{aligned} \tag{3.31}$$

Since $2\sin^2 x = 1 - \cos 2x$ we have

$$\begin{aligned} q(v^*) &= 1 - Dv^* \cos 2\Theta - 1 + \cos 2v^*\Theta \\ &= -Dv^* \cos 2\Theta + \sqrt{1-(\sin 2v^*\Theta)^2} \\ &= -Dv^* \cos 2\Theta + \sqrt{1-(Dv^* \sin 2\Theta)^2}. \end{aligned} \tag{3.32}$$

This is the second desired result (3.23).

It is interesting to find out the solutions $v^*$ at $\Theta = k\pi/4$ with $k = 1, 2, 3, 4$. $\Theta = \pi/4$ and $3\pi/4$ respond to the right angle and the L-shaped domains, and the numerical $v_k$ based on Theorem 3.1 are provided in Section 7.

When $\Theta = \pi/2, \pi$, we may obtain the real roots explicitly. When $\Theta = \pi/2$, we have $\sin\alpha\pi = 0$ from Theorem 3.1, and then $v^* = k$ to indicate that there is no singularity. When $\Theta = \pi$ denotes an interior crack within the plane, which is very important and interesting in both theory and computation. We have from Theorem 3.1 for $\beta = 0$, to yield

$$\sin 2\alpha\pi = \pm D\alpha \sin 2\pi = 0, \tag{3.33}$$

to give

$$\alpha = \frac{n}{2}, \quad n = 1, 2, \ldots . \tag{3.34}$$

Since $\Theta = \pi$, Eqs. (3.26) are violated, the particular solutions cannot be obtained directly from (3.24) and (3.25). We may derive the simplified singular solutions directly. From (3.4) we have the boundary conditions at $\Theta = \pi$

$$\begin{aligned} &\begin{pmatrix} -\sin v^*\pi + Dv^*\sin(v^*-2)\pi & \cos v^*\pi - Dv^*\cos(v^*-2)\pi & \sin v^*\pi & -\cos v^*\pi \\ \cos v^*\pi + Dv^*\cos(v^*-2)\pi & \sin v^*\pi + Dv^*\sin(v^*-2)\pi & \cos v^*\pi & \sin v^*\pi \\ \sin v^*\pi - Dv^*\sin(v^*-2)\pi & \cos v^*\pi - Dv^*\cos(v^*-2)\pi & -\sin v^*\pi & -\cos v^*\pi \\ \cos v^*\pi + Dv^*\cos(v^*-2)\pi & -\sin v^*\pi - Dv^*\sin(v^*-2)\pi & \cos v^*\pi & -\sin v^*\pi \end{pmatrix} \begin{pmatrix} a \\ b \\ c \\ d \end{pmatrix} \\ &= \begin{pmatrix} (-1+Dv^*)\sin v^*\pi & (1-Dv^*)\cos v^*\pi & \sin v^*\pi & -\cos v^*\pi \\ (1+Dv^*)\cos v^*\pi & (1+Dv^*)\sin v^*\pi & \cos v^*\pi & \sin v^*\pi \\ -(-1+Dv^*)\sin v^*\pi & (1-Dv^*)\cos v^*\pi & -\sin v^*\pi & -\cos v^*\pi \\ (1+Dv^*)\cos v^*\pi & -(1+Dv^*)\sin v^*\pi & \cos v^*\pi & -\sin v^*\pi \end{pmatrix} \begin{pmatrix} a \\ b \\ c \\ d \end{pmatrix} = \vec{0}. \end{aligned} \tag{3.35}$$

From (3.34), we may consider two cases of $v^* = n + \frac{1}{2}$ and $v^* = n$, respectively. First for $v^* = n + \frac{1}{2}$ we have from (3.35)

$$\begin{aligned} &\begin{pmatrix} (-1+Dv^*)\sin(n+\frac{1}{2})\pi & 0 & \sin(n+\frac{1}{2})\pi & 0 \\ 0 & (1+Dv^*)\sin(n+\frac{1}{2})\pi & 0 & \sin(n+\frac{1}{2})\pi \\ (1-Dv^*)\sin(n+\frac{1}{2})\pi & 0 & -\sin(n+\frac{1}{2})\pi & 0 \\ 0 & -(1+Dv^*)\sin(n+\frac{1}{2})\pi & 0 & -\sin(n+\frac{1}{2})\pi \end{pmatrix} \\ &\times \begin{pmatrix} a \\ b \\ c \\ d \end{pmatrix} = \vec{0}, \end{aligned} \tag{3.36}$$

to give the relations of coefficients

$$c = (1 - D(n+\tfrac{1}{2}))a, \quad d = -(1 + D(n+\tfrac{1}{2}))b \text{ for } v^* = n+\tfrac{1}{2}. \tag{3.37}$$

Please cite this article as: Li Z-C, et al. Models of corner and crack singularity of linear elastostatics and their numerical solutions. Eng Anal Bound Elem (2010), doi:10.1016/j.enganabound.2010.01.001

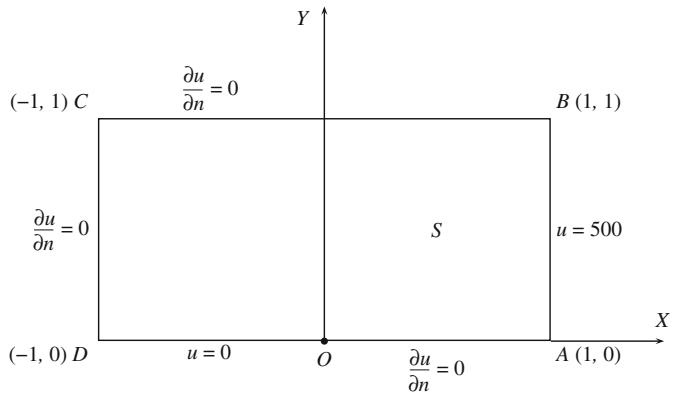


**Fig. 1.** Motz's problem.

Next for $v^*=n$ we have from (3.35)

$$\begin{pmatrix} 0 & (1-Dn)\cos n\pi & 0 & -\cos n\pi \\ (1+Dn)\cos n\pi & 0 & \cos n\pi & 0 \\ 0 & (1-Dn)\cos n\pi & 0 & -\cos n\pi \\ (1+Dn)\cos n\pi & 0 & \cos n\pi & 0 \end{pmatrix} \begin{pmatrix} a \\ b \\ c \\ d \end{pmatrix} = \vec{0}, \tag{3.38}$$

to give

$$c=-(1+Dn)a, \quad d=(1-Dn)b \ \text{ for } v^*=n. \tag{3.39}$$

By applying (3.37) and (3.39), the particular solutions in (3.2) and (3.3) are simplified as

$$\begin{aligned} u_L = &\sum_{n=0}^{L-1} r^{n+1/2}\left\{a_{2n+1}D\left(n+\frac{1}{2}\right)\left[-\sin\left(n+\frac{1}{2}\right)\theta+\sin\left(n-\frac{3}{2}\right)\theta\right]\right. \\ &+b_{2n+1}\left[\left(2+D\left(n+\frac{1}{2}\right)\right)\cos\left(n+\frac{1}{2}\right)\theta\right. \\ &\left.\left.-D\left(n+\frac{1}{2}\right)\cos\left(n-\frac{3}{2}\right)\theta\right]\right\} \\ &+\sum_{n=1}^{L} r^n\{a_{2n}[-(2+Dn)\sin n\theta+Dn\sin(n-2)\theta] \\ &+b_{2n}Dn[\cos n\theta-\cos(n-2)\theta]\}, \end{aligned} \tag{3.40}$$

$$\begin{aligned} v_L = &\sum_{n=0}^{L-1} r^{n+1/2}\left\{a_{2n+1}\left[\left(2-D\left(n+\frac{1}{2}\right)\right)\cos\left(n+\frac{1}{2}\right)\theta\right.\right. \\ &\left.+D\left(n+\frac{1}{2}\right)\cos\left(n-\frac{3}{2}\right)\theta\right]+b_{2n+1}D\left(n+\frac{1}{2}\right)\left[-\sin\left(n+\frac{1}{2}\right)\theta\right. \\ &\left.\left.+\sin\left(n-\frac{3}{2}\right)\theta\right]\right\}+\sum_{n=1}^{L} r^n\{a_{2n}Dn[-\cos n\theta+\cos(n-2)\theta] \\ &+b_{2n}[(2-Dn)\sin n\theta+Dn\sin(n-2)\theta]\}. \end{aligned} \tag{3.41}$$

## 4. Model A of crack singularity and its numerical solutions

### 4.1. Model A of crack singularity

Let us mimic Motz's problem of the Laplace equation satisfying the boundary conditions in Fig. 1 [23] for elastostatics. For the rectangle $S=\{(x,y)|-1\le x\le 1, 0\le y\le 1\}$, there exists a crack line $\overline{OD}$ under the clamped boundary conditions, and the symmetric boundary conditions on $\overline{OA}\cup\overline{BC}\cup\overline{CD}$. On $\overline{AB}$ we suppose that $u=1$ and no exterior force along the $y$ direction, which implies $\sigma_{xy}=u_y+v_x=0$.[2] Since $u_y=0$ on $\overline{AB}$, the condition $v_x=0$ is obtained. Then the Model A is designed as the Cauchy–Navier equation (2.5) satisfying the following boundary conditions:

$$u=v=0 \quad \text{on } \overline{OD}, \tag{4.1}$$

$$v=u_y=0 \quad \text{on } \overline{OA}\cup\overline{CB}, \tag{4.2}$$

$$u=v_x=0 \quad \text{on } \overline{CD}, \tag{4.3}$$

$$u=1, \quad v_x=0 \ \text{ on } \overline{AB}. \tag{4.4}$$

To satisfy the boundary condition on $\overline{OA}$ with $\theta=0$, for solution $u$ in (3.40) we have from $u_y=\partial u/r\partial\theta=0$, i.e.,

$$a_{2n+1}D(n+\tfrac{1}{2})[-(n+\tfrac{1}{2})+(n-\tfrac{3}{2})]=-a_{2n+1}D(2n+1)=0,$$

$$a_{2n}[-(2+Dn)n+Dn(n-2)]=-2n(D+1)a_{2n}+1=0. \tag{4.5}$$

Then we conclude $a_{2n+1}=a_{2n}=0$. Eqs. (3.40) and (3.41) lead to

$$\begin{aligned} u_L = &\sum_{n=0}^{L-1} b_{2n+1}r^{n+1/2}\left[\left(2+D\left(n+\frac{1}{2}\right)\right)\cos\left(n+\frac{1}{2}\right)\theta\right. \\ &\left.-D\left(n+\frac{1}{2}\right)\cos\left(n-\frac{3}{2}\right)\theta\right]+\sum_{n=1}^{L} b_{2n}r^n\{Dn[\cos n\theta-\cos(n-2)\theta]\}, \end{aligned} \tag{4.6}$$

$$\begin{aligned} v_L = &\sum_{n=0}^{L-1} b_{2n+1}r^{n+1/2}\left\{D\left(n+\frac{1}{2}\right)\left[-\sin\left(n+\frac{1}{2}\right)\theta+\sin\left(n-\frac{3}{2}\right)\theta\right]\right\} \\ &+\sum_{n=1}^{L} r^n b_{2n}\{(2-Dn)\sin n\theta+Dn\sin(n-2)\theta\}. \end{aligned} \tag{4.7}$$

Note that the number of unknown coefficients $b_k$ in (4.6) and (4.7) is $2L$ in $u_L$ and $v_L$. Model A of crack singularity is said to be *symmetric* if $u_y=v=0$, which implies that $u$ in (4.6) and $v$ in (4.7) are symmetric and anti-symmetric with respect to $\theta=0$, respectively. We may also design the anti-symmetric Model A, by replacing the boundary conditions on $\overline{OA}$ with

$$u=v_y=0 \quad \text{on } \overline{OA}. \tag{4.8}$$

### 4.2. The collocation Trefftz method

We will use the collocation method in [24] with the stability analysis [22].

We choose the particular solutions (4.6) and (4.7), and denote their set by $V_L$. Since they satisfy the governing equation (2.5) and the boundary conditions on $\overline{OD}\cup\overline{OA}$ in Fig. 1 already, the coefficients $a_k$ and $b_k$ are sought by satisfying the rest of boundary conditions in (4.2)–(4.4). Define the boundary energy

$$I(u,v)=\int_{\overline{AB}}[(u-1)^2+w^2v_x^2]+\int_{\overline{BC}}[v^2+w^2u_y^2]+\int_{\overline{CD}}[u^2+w^2v_x^2], \tag{4.9}$$

where $w$ is a weight. We choose $w=1/L$ in computation. The collocation Trefftz method (CTM) reads: To seek $(u_N,v_N)\in V_L$ such that

$$I(u_L,v_L)=\min_{(u,v)\in V_L} I(u,v). \tag{4.10}$$

When the integrals in (4.9) involve numerical integration approximation, the solutions are given by

$$\hat{I}(u_L,v_L)=\min_{(u,v)\in V_L} \hat{I}(u,v), \tag{4.11}$$

[2] We use the notations $u_y=\partial u/\partial y$ and $v_x=\partial v/\partial x$.

Please cite this article as: Li Z-C, et al. Models of corner and crack singularity of linear elastostatics and their numerical solutions. Eng Anal Bound Elem (2010), doi:10.1016/j.enganabound.2010.01.001

where

$$\hat{I}(u,v)=\hat{\int}_{\overline{AB}}[(u-1)^2+w^2v_x^2]+\hat{\int}_{\overline{BC}}[v^2+w^2u_y^2]+\hat{\int}_{\overline{CD}}[u^2+w^2v_x^2], \tag{4.12}$$

where $\hat{\int}$ is the numerical approximation of $\int$ by some integration rules, such as the central or the Gaussian quadrature.

We may establish the collocation equations of $u_L$ and $v_L$, to satisfy the rest of boundary conditions directly. Denote the basis particular solutions,

$$\Phi_{2n+1}(r,\theta)=r^{n+1/2}[(2+D(n+\tfrac{1}{2}))\cos(n+\tfrac{1}{2})\theta-D(n+\tfrac{1}{2})\cos(n-\tfrac{3}{2})\theta],$$

$$\Phi_{2n}(r,\theta)=r^nDn[\cos n\theta-\cos(n-2)\theta], \tag{4.13}$$

$$\Psi_{2n+1}(r,\theta)=r^{n+1/2}D(n+\tfrac{1}{2})[-\sin(n+\tfrac{1}{2})\theta+\sin(n-\tfrac{3}{2})\theta],$$

$$\Psi_{2n}(r,\theta)=r^n[(2-Dn)\sin n\theta+Dn\sin(n-2)\theta]. \tag{4.14}$$

Then the solutions (4.6) and (4.7) are denoted simply by

$$u_L=\sum_{n=1}^{2L}b_n\Phi_n(r,\theta),\quad v_L=\sum_{n=1}^{2L}b_n\Psi_n(r,\theta). \tag{4.15}$$

Let $\overline{AB}\cup\overline{BC}\cup\overline{CD}$ be divided uniformly into small sections with length $h$. Denote $h=1/N$. On $\overline{AB}$, let $Q_i=(r_i,\theta_i)$ denote the middle nodes of the small sections, we may have the following collocation equations from (4.4) and (4.15)

$$\sqrt{h}\sum_{n=1}^{2L}b_n\Phi_n(r_i,\theta_i)=\sqrt{h}\quad (r_i,\theta_i)\in\overline{AB}, \tag{4.16}$$

$$w\sqrt{h}\sum_{n=1}^{2L}b_n\frac{\partial}{\partial x}\Psi_n(r_i,\theta_i)=0\quad (r_i,\theta_i)\in\overline{AB}, \tag{4.17}$$

where $w$ is a weight constant to balance two kinds of collocation equations. Similarly, from (4.2) and (4.3), we obtain the collocation equations on $\overline{CB}\cup\overline{CD}$,

$$w\sqrt{h}\sum_{n=1}^{2L}b_n\frac{\partial}{\partial y}\Phi_n(r_i,\theta_i)=0\quad (r_i,\theta_i)\in\overline{BC}, \tag{4.18}$$

$$\sqrt{h}\sum_{n=1}^{2L}b_n\Psi_n(r_i,\theta_i)=0\quad (r_i,\theta_i)\in\overline{BC}, \tag{4.19}$$

$$\sqrt{h}\sum_{n=1}^{2L}b_n\Phi_n(r_i,\theta_i)=0\quad (r_i,\theta_i)\in\overline{CD}, \tag{4.20}$$

$$w\sqrt{h}\sum_{n=1}^{2L}b_n\frac{\partial}{\partial x}\Psi_n(r_i,\theta_i)=0,\quad (r_i,\theta_i)\in\overline{CD}. \tag{4.21}$$

Eqs. (4.16)–(4.21) form the linear algebraic equations,

$$\mathbf{Fx}=\mathbf{b}, \tag{4.22}$$

where $\mathbf{F}\in R^{m\times 2L}$, $\mathbf{x}\in 2L$, $\mathbf{b}\in R^m$, $m=8M$, and $M$ is the number of collocation nodes on $\overline{AB}$. We always choose $m>2L$ in computation. Hence Eq. (4.22) is the system of over-determined equations. We may choose the least squares method or the QR factorization, to seek the coefficient vector $\mathbf{x}=\{b_1,b_2,\ldots,b_{2L}\}^T$. The CTM is studied in [24] for Poisson's, biharmonic and Helmholtz equations, as well as eigenvalue problems. This paper is the first one to apply the CTM for elastostatics problems. Following [24,31], the equivalence between (4.11) and (4.22) can be proven, and error bounds may also be derived. Details will appear elsewhere.

To measure numerical stability, we compute the condition number of (4.22) by

$$\mathrm{Cond}=\frac{\sigma_{max}}{\sigma_{min}}, \tag{4.23}$$

where $\sigma_{max}$ and $\sigma_{min}$ are the maximal and the minimal singular values of matrix $\mathbf{F}$, respectively. A better criterion of numerical stability is given by the effective condition number in Li et al. [21], defined by

$$\mathrm{Cond_e ff}=\frac{\|\mathbf{b}\|}{\sigma_{min}\|\mathbf{x}\|}, \tag{4.24}$$

where $\|\mathbf{x}\|$ and $\|\mathbf{b}\|$ are 2-norms.

### 4.3. Numerical results

We choose $\lambda=\mu=1$, the constant $D=\frac{1}{2}$ and $\frac{5}{11}$ for the plane strain and the plane stress problems, respectively. Errors, condition numbers and the leading coefficients $b_1$ and $b_2$ are listed in Tables 1 and 2, where $\delta(u)=u_L-u$ and $\delta(v)=v_L-v$. All tables of this paper are calculated by double precision. Table 3 lists the results of different $M$ for $D=\frac{1}{2}$ and $L=20$, to find a good choice at $M=15$. By using such a good matching: $M=\frac{3}{4}L$, the results are given in Tables 1 and 2. From Tables 1 and 2 we can see the asymptotes

$$\|\varepsilon\|_B=O(0.56^L),\quad \|\delta(u)\|_{\infty,\overline{AB}\cup\overline{CD}}=O(0.58^L),\quad \|\delta(v)\|_{\infty,\overline{BC}}=O(0.58^L), \tag{4.25}$$

$$\mathrm{Cond}=O(1.48^L),\quad \mathrm{Cond_e ff}=O(1.06^L). \tag{4.26}$$

In Tables 4 and 5, we list the coefficients $b_i$, where the digits in bold denote the significant digits, compared with the higher accuracy of $b_i$ obtained by using $L=200$ with 500 working digits. From Tables 4 and 5, we find that the crucial leading coefficient $b_1$ has 14 significant digits.

## 5. Singular solutions near corners under free stress boundary conditions

For clamped boundary conditions the corner singularity of elasticity plane in Sections 3 and 4 are new. For free stress boundary conditions the corner singularity of elasticity plane was first discussed in Williams [38], and then in Lin and Tong [28], Jirousek and Wroblewski [15], Jirousek and Venkstesh [14] and Qin [36]. In this section, we consider only the symmetric case of the corner with $\theta\in[0,\pm\Theta]$ for the sectorial domain $S=\{(r,\theta)|0\le R,0\le\theta\le\Theta\}$, where $\Theta\in(0,\pi]$. The boundary conditions are given as follows:

$$u_y=v=0\quad \text{at } \theta=0, \tag{5.1}$$

$$\tau_x=\tau_y=0\quad \text{at } \theta=\Theta, \tag{5.2}$$

where the stress formulas are given by

$$\tau_x=\sigma_x\cos(n,x)+\sigma_{xy}\cos(n,y), \tag{5.3}$$

$$\tau_y=\sigma_{xy}\cos(n,x)+\sigma_y\cos(n,y), \tag{5.4}$$

where $\sigma_x=\sigma_{11},\sigma_y=\sigma_{22}$ and $\sigma_{xy}=\sigma_{12}=\sigma_{21}$ as in (2.3). For the exterior normal $\vec{n}$ of the edge boundary, we have

$$\cos(n,x)=\cos\left(\frac{\pi}{2}+\theta\right)=-\sin\theta,\quad \cos(n,y)=\cos\theta. \tag{5.5}$$

Hence we have from (5.3) and (5.4)

$$\tau_x=-\sigma_x\sin\theta+\sigma_{xy}\cos\theta=0,\quad \tau_y=-\sigma_{xy}\sin\theta+\sigma_y\cos\theta=0. \tag{5.6}$$

We will use different approaches from those in Sections 3 and 4, to seek the particular solutions of (3.2) and (3.3) satisfying the boundary conditions (5.1) and (5.6).

First, let us give a lemma from calculus.

Please cite this article as: Li Z-C, et al. Models of corner and crack singularity of linear elastostatics and their numerical solutions. Eng Anal Bound Elem (2010), doi:10.1016/j.enganabound.2010.01.001

**Table 1**
Errors, condition numbers and the leading coefficients $b_1$ and $b_2$ for Model A by the CTM as $D=\frac{1}{2}$.

| $M$ | $L$ | $\|\varepsilon\|_B$ | $\|\delta(u)\|_{\infty,\overline{AB}\cup\overline{CD}}$ | $\|\delta(v)\|_{\infty,\overline{BC}}$ | Cond | Cond_eff | $b_1$ | $b_2$ |
|---|---|---|---|---|---|---|---|---|
| 3 | 4 | 1.11(−2) | 1.11(−2) | 3.23(−3) | 1.10(1) | 1.72 | 4.10251982712500(−1) | 2.50698260629164(−1) |
| 6 | 8 | 6.79(−4) | 7.35(−4) | 3.21(−4) | 8.23(1) | 2.35 | 4.10654626510859(−1) | 2.51537941297936(−1) |
| 9 | 12 | 5.53(−5) | 6.11(−5) | 3.69(−5) | 6.09(2) | 3.54 | 4.10647631047238(−1) | 2.51569676360375(−1) |
| 12 | 16 | 4.96(−6) | 5.50(−6) | 3.57(−6) | 3.93(3) | 4.92 | 4.10647315855802(−1) | 2.51571034567718(−1) |
| 15 | 20 | 4.74(−7) | 5.56(−7) | 3.99(−7) | 2.29(4) | 6.38 | 4.10647274208211(−1) | 2.51571057835755(−1) |
| 18 | 24 | 4.68(−8) | 6.12(−8) | 4.55(−8) | 1.24(5) | 7.88 | 4.10647272484115(−1) | 2.51571061809156(−1) |
| 21 | 28 | 4.72(−9) | 6.83(−9) | 5.28(−9) | 6.43(5) | 9.41 | 4.10647272270177(−1) | 2.51571061743769(−1) |
| 24 | 32 | 4.84(−10) | 7.60(−10) | 6.13(−10) | 3.21(6) | 11 | 4.10647272267430(−1) | 2.51571061764127(−1) |
| 27 | 36 | 5.01(−11) | 8.59(−11) | 7.11(−11) | 1.56(7) | 12.5 | 4.10647272266421(−1) | 2.51571061762613(−1) |
| 30 | 40 | 5.25(−12) | 9.84(−12) | 8.23(−12) | 7.41(7) | 14.1 | 4.10647272266494(−1) | 2.51571061762734(−1) |

**Table 2**
Errors, condition numbers and the leading coefficients $b_1$ and $b_2$ for Model A by the CTM as $D=\frac{5}{11}$.

| $M$ | $L$ | $\|\varepsilon\|_B$ | $\|\delta(u)\|_{\infty,\overline{AB}\cup\overline{CD}}$ | $\|\delta(v)\|_{\infty,\overline{BC}}$ | Cond | Cond_eff | $b_1$ | $b_2$ |
|---|---|---|---|---|---|---|---|---|
| 3 | 4 | 1.11(−2) | 1.19(−2) | 2.92(−3) | 9.27 | 1.63 | 4.07637079571382(−1) | 2.08971959209034(−1) |
| 6 | 8 | 6.33(−4) | 6.98(−4) | 2.88(−4) | 7.02(1) | 2.3 | 4.07798355978068(−1) | 2.09715764414755(−1) |
| 9 | 12 | 5.10(−5) | 5.76(−5) | 3.39(−5) | 5.16(2) | 3.46 | 4.07792974425139(−1) | 2.09740315069872(−1) |
| 12 | 16 | 4.56(−6) | 5.17(−6) | 3.27(−6) | 3.32(3) | 4.79 | 4.07792708870668(−1) | 2.09741269589606(−1) |
| 15 | 20 | 4.35(−7) | 5.16(−7) | 3.62(−7) | 1.93(4) | 6.21 | 4.07792671891129(−1) | 2.09741282540668(−1) |
| 18 | 24 | 4.29(−8) | 5.51(−8) | 4.11(−8) | 1.05(5) | 7.68 | 4.07792670357375(−1) | 2.09741285227151(−1) |
| 21 | 28 | 4.33(−9) | 6.21(−9) | 4.77(−9) | 5.44(5) | 9.17 | 4.07792670157548(−1) | 2.09741285168149(−1) |
| 24 | 32 | 4.43(−10) | 6.95(−10) | 5.55(−10) | 2.72(6) | 10.7 | 4.07792670153856(−1) | 2.09741285183747(−1) |
| 27 | 36 | 4.59(−11) | 7.78(−11) | 6.46(−11) | 1.32(7) | 12.2 | 4.07792670152782(−1) | 2.09741285182719(−1) |
| 30 | 40 | 4.80(−12) | 8.93(−12) | 7.50(−12) | 6.28(7) | 13.7 | 4.07792670152828(−1) | 2.09741285182831(−1) |

**Table 3**
Errors, condition numbers and the leading coefficients $b_1$ and $b_2$ for model A by the CTM as $D=\frac{1}{2}$ and $L=20$.

| $M$ | $\|\varepsilon\|_B$ | $\|\delta(u)\|_{\infty,\overline{AB}\cup\overline{CD}}$ | $\|\delta(v)\|_{\infty,\overline{BC}}$ | Cond | Cond_eff | $b_1$ | $b_2$ |
|---|---|---|---|---|---|---|---|
| 6 | 2.57(−7) | 4.67(−6) | 2.55(−6) | 2.21(4) | 6.58 | 4.10647249074947(−1) | 2.51571038577816(−1) |
| 9 | 4.30(−7) | 1.25(−6) | 8.18(−7) | 2.26(4) | 6.41 | 4.10647271576030(−1) | 2.51571053945849(−1) |
| 12 | 4.63(−7) | 7.22(−7) | 5.12(−7) | 2.28(4) | 6.39 | 4.10647273644057(−1) | 2.51571056781410(−1) |
| 15 | 4.74(−7) | 5.56(−7) | 3.99(−7) | 2.29(4) | 6.38 | 4.10647274208211(−1) | 2.51571057835755(−1) |
| 18 | 4.80(−7) | 5.28(−7) | 3.51(−7) | 2.29(4) | 6.38 | 4.10647274441860(−1) | 2.51571058364345(−1) |
| 21 | 4.83(−7) | 5.14(−7) | 3.54(−7) | 2.30(4) | 6.37 | 4.10647274561803(−1) | 2.51571058671756(−1) |
| 24 | 4.85(−7) | 5.06(−7) | 3.55(−7) | 2.30(4) | 6.37 | 4.10647274631963(−1) | 2.51571058867490(−1) |
| 27 | 4.86(−7) | 5.01(−7) | 3.56(−7) | 2.30(4) | 6.37 | 4.10647274676761(−1) | 2.51571059000162(−1) |
| 30 | 4.87(−7) | 4.97(−7) | 3.57(−7) | 2.30(4) | 6.37 | 4.10647274707216(−1) | 2.51571059094364(−1) |
| 33 | 4.88(−7) | 4.94(−7) | 3.57(−7) | 2.30(4) | 6.37 | 4.10647274728920(−1) | 2.51571059163711(−1) |

**Table 4**
The leading coefficients for Model A by the CTM as $D=\frac{1}{2}$ and $L=40$, where "Sig." denotes the number of significant digits.

| $i$ | All digits | Sig. | $i$ | All digits | Sig. |
|---|---|---|---|---|---|
| 1 | **4.10647272266649**4(−1) | 14 | 41 | **6.6**6203785143277(−10) | 2 |
| 2 | **2.51571061762734**(−1) | 13 | 42 | **1.1594**5989171034(−8) | 5 |
| 3 | **9.38402559696613**(−2) | 15 | 43 | −**9.60**0090044002850(−9) | 3 |
| 4 | **3.07049108695**358(−2) | 12 | 44 | **6.04**311295359092(−9) | 3 |
| 5 | −**1.33072821410**658(−2) | 13 | 45 | −**1.76**376133662528(−10) | 3 |
| 6 | −**2.60551082272**462(−3) | 11 | 46 | −**2.78**038068295960(−9) | 3 |
| 7 | **8.91754903117**311(−3) | 11 | 47 | **2.8**3403346078824(−9) | 2 |
| 8 | −**6.69374333311**149(−3) | 11 | 48 | −**1.44**186153642238(−9) | 3 |
| 9 | **3.641352**35015083(−6) | 7 | 49 | **3**.144760548026870(−11) | 1 |
| 10 | **1.327976031**64819(−3) | 10 | 50 | **6.6**7848883183302(−10) | 2 |
| 11 | −**3.938511246**49121(−4) | 10 | 51 | −**5.7**0188229184457(−10) | 2 |
| 12 | **8.379253228**44148(−4) | 10 | 52 | **3**.44387135360899(−10) | 1 |
| 13 | −**2.9945641**6826879(−6) | 8 | 53 | −**8**.58589386862836(−12) | 1 |
| 14 | −**3.524298649**03714(−4) | 10 | 54 | −**1.5**9990818166583(−10) | 2 |
| 15 | **3.24690762**531300(−4) | 9 | 55 | **1.6**2417585401824(−10) | 2 |
| 16 | −**1.57456292**034103(−4) | 9 | 56 | −**8**.21171983972912(−11) | 1 |

Please cite this article as: Li Z-C, et al. Models of corner and crack singularity of linear elastostatics and their numerical solutions. Eng Anal Bound Elem (2010), doi:10.1016/j.enganabound.2010.01.001

Table 4 (*continued*)

| *i* | All digits | Sig. | *i* | All digits | Sig. |
|---|---|---|---|---|---|
| 17 | −**8.0632324**0445713(−8) | 8 | 57 | 1.32661996826598(−12) | 0 |
| 18 | **7.1312497**6192084(−5) | 8 | 58 | **3**.84098467576664(−11) | 1 |
| 19 | −**4.0820460**3518075(−5) | 8 | 59 | −**3**.30585176206119(−11) | 1 |
| 20 | **3.8693654**4039162(−5) | 9 | 60 | **1**.90642054386328(−11) | 1 |
| 21 | −**3.3745677**5389799(−6) | 8 | 61 | −2.76785227660824(−13) | 0 |
| 22 | −**1.5371541**8109543(−5) | 9 | 62 | −**8**.85386594129221(−12) | 1 |
| 23 | **1.6584936**8076219(−5) | 8 | 63 | 8.82299324111171(−12) | 0 |
| 24 | −**8.794074**62804704(−6) | 7 | 64 | −4.35547407571365(−12) | 0 |
| 25 | **3.557979**30227532(−7) | 7 | 65 | 1.09378835982087(−14) | 0 |
| 26 | **3.669417**29535458(−6) | 7 | 66 | **2**.03763392558782(−12) | 1 |
| 27 | −**2.65431**844360349(−6) | 6 | 67 | −**1**.68106310329655(−12) | 1 |
| 28 | **1.962511**64309636(−6) | 7 | 68 | 8.69138399475569(−13) | 0 |
| 29 | −**7.4457**9741160189(−8) | 5 | 69 | 2.96650892492666(−14) | 0 |
| 30 | −**8.73166**822322096(−7) | 6 | 70 | −3.98231056553442(−13) | 0 |
| 31 | **8.9188**1164790093(−7) | 5 | 71 | 3.59990602781704(−13) | 0 |
| 32 | −**4.5564**1167759193(−7) | 5 | 72 | −1.61383266794306(−13) | 0 |
| 33 | **1.1991**9047833575(−8) | 5 | 73 | −2.52343313378514(−15) | 0 |
| 34 | **2.04817**784788004(−7) | 6 | 74 | 7.17469564382971(−14) | 0 |
| 35 | −**1.6076**2427325796(−7) | 5 | 75 | −5.29166570542841(−14) | 0 |
| 36 | **1.07730**530862914(−7) | 6 | 76 | 2.03478061859853(−14) | 0 |
| 37 | −**4.0490**7284800504(−9) | 5 | 77 | 4.94681464457029(−15) | 0 |
| 38 | −**4.848**32287196653(−8) | 4 | 78 | −9.46006769817745(−15) | 0 |
| 39 | **4.977**24966182189(−8) | 4 | 79 | 5.00214195594415(−15) | 0 |
| 40 | −**2.54**740240872724(−8) | 3 | 80 | −8.07198239900287(−16) | 0 |

**Table 5**
The leading coefficients for Model A by the CTM as $D=\frac{5}{11}$ and $L=40$, where "Sig." denotes the number of significant digits.

| *i* | All digits | Sig. | *i* | All digits | Sig. |
|---|---|---|---|---|---|
| 1 | **4.07792670152828**(−1) | 14 | 41 | **6.0**5177310086391(−10) | 2 |
| 2 | **2.09741285182831**(−1) | 13 | 42 | **1.045**36619410337(−8) | 4 |
| 3 | **9.62856103741701**(−2) | 13 | 43 | −**8.46**189297869868(−9) | 3 |
| 4 | **2.76183879928**471(−2) | 12 | 44 | **5.46**078789055957(−9) | 3 |
| 5 | −**1.19762989485270**(−2) | 13 | 45 | −**1.648**27249646381(−10) | 4 |
| 6 | −**2.335097629**08167(−3) | 11 | 46 | −**2.50**707482281544(−9) | 3 |
| 7 | **8.01687784228**362(−3) | 11 | 47 | **2.55**828004544452(−9) | 3 |
| 8 | −**6.022814344**61713(−3) | 11 | 48 | −**1.30**289694456698(−9) | 3 |
| 9 | −**1.4913065**7247683(−4) | 9 | 49 | **2.8**8341445649076(−11) | 2 |
| 10 | **1.190339081**30327(−3) | 11 | 50 | **6.0**2263711566840(−10) | 2 |
| 11 | −**2.33838564**513919(−4) | 10 | 51 | −**5**.04926183157911(−10) | 1 |
| 12 | **7.55317190**747609(−4) | 10 | 52 | **3.1**1217597658468(−10) | 2 |
| 13 | −**4.6781818**8128383(−6) | 8 | 53 | −**8**.07135498822367(−12) | 1 |
| 14 | −**3.160764775**11216(−4) | 10 | 54 | −**1**.44261350147204(−10) | 1 |
| 15 | **2.922743396**87023(−4) | 10 | 55 | **1.4**6628619946623(−10) | 2 |
| 16 | −**1.423088876**70281(−4) | 10 | 56 | −7.42282143061901(−11) | 0 |
| 17 | −**9.27204**750148185(−8) | 6 | 57 | 1.25995634010131(−12) | 0 |
| 18 | **6.4045031**0193123(−5) | 8 | 58 | 3.46340109145301(−11) | 0 |
| 19 | −**3.3890882**5256940(−5) | 9 | 59 | −**2**.93769250151829(−11) | 1 |
| 20 | **3.4993477**6471675(−5) | 9 | 60 | **1**.72565018449597(−11) | 1 |
| 21 | −**3.131385**20671870(−6) | 7 | 61 | −2.89465586997051(−13) | 0 |
| 22 | −**1.3828986**9832243(−5) | 8 | 62 | −7.97136045559816(−12) | 0 |
| 23 | **1.4965302**7384342(−5) | 8 | 63 | 7.96654251154383(−12) | 0 |
| 24 | −**7.952409**17059638(−6) | 7 | 64 | −**3**.94305407358385(−12) | 1 |
| 25 | **3.121509**40793412(−7) | 7 | 65 | 2.04069440948681(−14) | 0 |
| 26 | **3.304507**98386428(−6) | 7 | 66 | **1**.83503653391467(−12) | 1 |
| 27 | −**2.289205**07763688(−6) | 7 | 67 | −1.49968276847398(−12) | 0 |
| 28 | **1.774299**04226567(−6) | 7 | 68 | 7.93632735452351(−13) | 0 |
| 29 | −**7.01146**877282463(−8) | 6 | 69 | 1.95426543505334(−14) | 0 |
| 30 | −**7.86691**120596366(−7) | 6 | 70 | −3.55692004814227(−13) | 0 |
| 31 | **8.04971**808535152(−7) | 6 | 71 | 3.24815277110125(−13) | 0 |
| 32 | −**4.1186**5176466270(−7) | 5 | 72 | −1.46421721827824(−13) | 0 |
| 33 | **1.083**94196959857(−8) | 4 | 73 | −1.40547698795339(−15) | 0 |
| 34 | **1.84587**751771489(−7) | 6 | 74 | 6.44070271052293(−14) | 0 |
| 35 | −**1.4064**3173854669(−7) | 5 | 75 | −4.74784256728221(−14) | 0 |
| 36 | **9.736**72023784266(−8) | 4 | 76 | 1.91906722780754(−14) | 0 |
| 37 | −**3.776**58521611431(−9) | 4 | 77 | 3.80036316303079(−15) | 0 |
| 38 | −**4.3704**6290153343(−8) | 5 | 78 | −8.19514263828618(−15) | 0 |
| 39 | **4.492**71969353005(−8) | 4 | 79 | 4.46795073904157(−15) | 0 |
| 40 | −**2.302**12113988927(−8) | 4 | 80 | −7.19945688720858(−16) | 0 |

Please cite this article as: Li Z-C, et al. Models of corner and crack singularity of linear elastostatics and their numerical solutions. Eng Anal Bound Elem (2010), doi:10.1016/j.enganabound.2010.01.001

**Lemma 5.1.** *There exist the equalities,*

$$\frac{\partial r}{\partial x}=\cos\theta,\quad \frac{\partial r}{\partial y}=\sin\theta,$$

$$\frac{\partial \theta}{\partial x}=-\frac{\sin\theta}{r},\quad \frac{\partial \theta}{\partial y}=\frac{\cos\theta}{r}. \tag{5.7}$$

**Lemma 5.2.** *For the solutions* (3.2) *and* (3.3) *satisfying* (5.1), *the stress tensors* $\tau_x$ *and* $\tau_y$ *at* $\theta\in(0,\Theta]$ *are given by*

$$\tau_x=2\mu\sum_{k=1}^{L}v_k r^{v_k-1}\{b_k[Dv_k\sin(v_k-2)\theta-D\sin v_k\theta]+d_k\sin v_k\theta\}, \tag{5.8}$$

$$\tau_y=2\mu\sum_{k=1}^{L}v_k r^{v_k-1}\{b_k[Dv_k\cos(v_k-2)\theta+D\cos v_k\theta]+d_k\cos v_k\theta\}. \tag{5.9}$$

**Proof.** Since

$$u_y=\frac{\partial u}{\partial y}=\frac{\partial u}{\partial r}\frac{\partial r}{\partial y}+\frac{\partial u}{\partial \theta}\frac{\partial \theta}{\partial y}, \tag{5.10}$$

we have from (3.2) and Lemma 5.1

$$\begin{aligned}u_y=\sum_{k=1}^{L}v_k r^{v_k-1}\{&a_k[-\cos(v_k-1)\theta+Dv_k\cos(v_k-3)\theta\\&-2D\cos(v_k-2)\theta\cos\theta]+b_k[-\sin(v_k-1)\theta+Dv_k\sin(v_k-3)\theta\\&-2D\sin(v_k-2)\theta\cos\theta]+c_k\cos(v_k-1)\theta+d_k\sin(v_k-1)\theta\}.\end{aligned} \tag{5.11}$$

When $u_y=\partial u/r\partial\theta|_{\theta=0}=0$ we obtain

$$\sum_{k=1}^{L}v_k r^{v_k-1}\{a_k[-1+Dv_k-2D]+c_k\}=0, \tag{5.12}$$

to give

$$c_k=-(-1+Dv_k-2D)a_k,\quad k=1,2\ldots. \tag{5.13}$$

On the other hand, when the boundary condition $v=0|_{\theta=0}$, we have from (3.3)

$$c_0=0,\quad c_k=-(1+Dv_k)a_k,\quad k=1,2,\ldots. \tag{5.14}$$

Eqs. (5.13) and (5.14) lead to

$$c_k=a_k=0,\quad \forall k. \tag{5.15}$$

From (5.15), the particular solutions in (3.2) and (3.3) are simplified to

$$u_L=\sum_{k=1}^{L}r^{v_k}\{b_k[\cos v_k\theta-Dv_k\cos(v_k-2)\theta]-d_k\cos v_k\theta\}+d_0, \tag{5.16}$$

$$v_L=\sum_{k=1}^{L}r^{v_k}\{b_k[\sin v_k\theta+Dv_k\sin(v_k-2)\theta]+d_k\sin v_k\theta\}. \tag{5.17}$$

Next, based on Lemma 5.1, we have from (5.10) and (5.16)

$$\begin{aligned}u_y&=\sum_{k=1}^{L}v_k r^{v_k-1}\{b_k[-\sin(v_k-1)\theta+Dv_k\sin(v_k-3)\theta\\&\quad-2D\sin(v_k-2)\theta\cos\theta]+d_k\sin(v_k-1)\theta\}\\&=\sum_{k=1}^{L}v_k r^{v_k-1}\{b_k[-(1+D)\sin(v_k-1)\theta+D(v_k-1)\sin(v_k-3)\theta]\\&\quad+d_k\sin(v_k-1)\theta\},\end{aligned} \tag{5.18}$$

where we have used $2\sin(v_k-2)\theta\cos\theta=\sin(v_k-1)\theta+\sin(v_k-3)\theta$. Similarly, we have

$$\begin{aligned}v_x&=\sum_{k=1}^{L}v_k r^{v_k-1}\{b_k[\sin(v_k-1)\theta+Dv_k\sin(v_k-3)\theta\\&\quad+2D\cos(v_k-2)\theta\sin\theta]+d_k\sin(v_k-1)\theta\}\\&=\sum_{k=1}^{L}v_k r^{v_k-1}\{b_k[(1+D)\sin(v_k-1)\theta+D(v_k-1)\sin(v_k-3)\theta]\\&\quad+d_k\sin(v_k-1)\theta\}.\end{aligned} \tag{5.19}$$

Then the stress is given by

$$\begin{aligned}\sigma_{xy}&=\sigma_{12}\\&=\mu(u_y+v_x)\\&=2\mu\sum_{k=1}^{L}v_k r^{v_k-1}\{b_k[(D(v_k-1))\sin(v_k-3)\theta]+d_k\sin(v_k-1)\theta\}.\end{aligned} \tag{5.20}$$

Third, based on Lemma 5.1, we have from (5.16) and (5.17)

$$\begin{aligned}u_x&=\sum_{k=1}^{L}v_k r^{v_k-1}\{b_k[\cos(v_k-1)\theta-Dv_k\cos(v_k-3)\theta\\&\quad+2D\sin(v_k-2)\theta\sin\theta]-d_k\cos(v_k-1)\theta\}\\&=\sum_{k=1}^{L}v_k r^{v_k-1}\{b_k[(1-D)\cos(v_k-1)\theta-D(v_k-1)\cos(v_k-3)\theta]\\&\quad-d_k\cos(v_k-1)\theta,\end{aligned} \tag{5.21}$$

$$\begin{aligned}v_y&=\sum_{k=1}^{L}v_k r^{v_k-1}\{b_k[\cos(v_k-1)\theta+Dv_k\cos(v_k-3)\theta\\&\quad-2D\cos(v_k-2)\theta\cos\theta]+d_k\cos(v_k-1)\theta\}\\&=\sum_{k=1}^{L}v_k r^{v_k-1}\{b_k[(1-D)\cos(v_k-1)\theta+D(v_k-1)\cos(v_k-3)\theta]\\&\quad+d_k\cos(v_k-1)\theta\}.\end{aligned} \tag{5.22}$$

Then we have (5.21) and (5.22)

$$\begin{aligned}\sigma_x&=\sigma_{11}\\&=(\lambda+2\mu)u_x+\lambda v_y\\&=2\sum_{k=1}^{L}v_k r^{v_k-1}\{b_k[(\lambda+\mu)(1-D))\cos(v_k-1)\theta\\&\quad-\mu D(v_k-1)\cos(v_k-3)\theta]-d_k[\mu\cos(v_k-1)\theta]\},\end{aligned} \tag{5.23}$$

and

$$\begin{aligned}\sigma_y&=\sigma_{22}=\lambda u_x+(\lambda+2\mu)v_y\\&=2\sum_{k=1}^{L}v_k r^{v_k-1}\{b_k[(\lambda+\mu)(1-D)\cos(v_k-1)\theta\\&\quad+\mu D(v_k-1)\cos(v_k-3)\theta]+d_k[\mu\cos(v_k-1)\theta]\}.\end{aligned} \tag{5.24}$$

Therefore, we have (5.20) and (5.23)

$$\begin{aligned}\tau_x&=-\sigma_x\sin\theta+\sigma_{xy}\cos\theta\\&=2\sum_{k=1}^{L}v_k r^{v_k-1}\{b_k[(-\lambda(1-D)-\mu(1-D))\cos(v_k-1)\theta\sin\theta\\&\quad+\mu D(v_k-1)\sin(v_k-2)\theta]+d_k\mu\sin v_k\theta\}.\end{aligned} \tag{5.25}$$

From $D=(\lambda+\mu)/(\lambda+3\mu)$, there exists the equality

$$\lambda(1-D)=\mu(3D-1). \tag{5.26}$$

Eq. (5.25) is reduced to

$$\begin{aligned}\tau_x=2\mu\sum_{k=1}^{L}v_k r^{v_k-1}\{&b_k[-2D\cos(v_k-1)\theta\sin\theta\\&+D(v_k-1)\sin(v_k-2)\theta]+d_k\sin v_k\theta\}\end{aligned}$$

Please cite this article as: Li Z-C, et al. Models of corner and crack singularity of linear elastostatics and their numerical solutions. Eng Anal Bound Elem (2010), doi:10.1016/j.enganabound.2010.01.001

$$= 2\mu \sum_{k=1}^{L} v_k r^{v_k-1}\{b_k[Dv_k \sin(v_k-2)\theta - D\sin v_k\theta] + d_k \sin v_k\theta\}. \tag{5.27}$$

This is the first desired result (5.8).

From (5.20), (5.24) and (5.26), we have similarly

$$\begin{aligned}\tau_y &= -\sigma_{xy}\sin\theta + \sigma_y\cos\theta \\ &= 2\sum_{k=1}^{L} v_k r^{v_k-1}\{b_k[(\lambda(1-D)+\mu(1-D))\cos(v_k-1)\theta\cos\theta \\ &\quad + \mu D(v_k-1)\cos(v_k-2)\theta] + d_k\mu\cos v_k\theta\} \\ &= 2\mu\sum_{k=1}^{L} v_k r^{v_k-1}\{b_k[D\cos(v_k-1)\theta\cos\theta \\ &\quad + 2D(v_k-1)\cos(v_k-2)\theta] + d_k\cos v_k\theta\} \\ &= 2\mu\sum_{k=1}^{L} v_k r^{v_k-1}\{b_k[Dv_k\cos(v_k-2)\theta + D\cos v_k\theta] + d_k\cos v_k\theta\}.\end{aligned} \tag{5.28}$$

This is the second desired result (5.9), and completes the proof of Lemma 5.2. □

**Theorem 5.1.** *For* (5.1) *and* (5.2) *with symmetric cases there exists the equality*,

$$\sin 2v^*\Theta = -v^*\sin 2\Theta. \tag{5.29}$$

**Proof.** Based on Lemma 5.2, the nonzero coefficients $b_k$ and $d_k$ in $\tau_x = \tau_y = 0$ exist if and only if the coefficient determinant in (5.8) and (5.9) is zero, to give

$$\begin{aligned}&[Dv_k\sin(v_k-2)\theta - D\sin v_k\theta] \\ &\quad \times \cos v_k\theta - [Dv_k\cos(v_k-2)\theta + D\cos v_k\theta] \times \sin v_k\theta = 0.\end{aligned} \tag{5.30}$$

This yields

$$\begin{aligned}&v_k[\sin(v_k-2)\theta\cos v_k\theta - \cos(v_k-2)\theta\sin v_k\theta] - \sin 2v_k\theta \\ &\quad = -v_k\sin 2\theta - \sin 2v_k\theta = 0.\end{aligned} \tag{5.31}$$

This is the desired result (5.29), and completes the proof of Theorem 5.1. □

In fact, Eq. (5.29) corresponds to the symmetric model with (5.16) and (5.17), and the following equation:

$$\sin 2v^*\Theta = v^*\sin 2\Theta \tag{5.32}$$

corresponds to the nonsymmetric model with $v_y = u = 0$ at $\theta = 0$. The particular solutions can also be obtained similarly, and the proof techniques are similar. Eqs. (5.29) and (5.32) coincide with [28]. Note that the signs corresponding the symmetry and anti-symmetry in Theorem 5.1 for the free stress boundary at $\theta = \Theta$ are just opposite to those in Theorem 3.1 for the clamped boundary conditions on $\theta = \Theta$.

Compared with Theorem 3.1, since $D \in (0,1)$, it is easy to see that the minimal real root of (3.13) are larger than that of (5.29) and (5.32). This coincides with the fact that the clamped boundary condition is a kind of constraints, so that the minimal eigenvalue from (3.13) will be larger.

**Remark 5.1.** Although Lemma 5.2 and Theorem 5.1 are derived for the plane strain problem, they are still valid for the plane stress problems, since for the latter case, only the Lamé constants $\lambda$ is replaced by $\lambda' = 2\lambda\mu/(\lambda+2\mu)$ (see [40]).

**Remark 5.2.** Note that in Section 3 and this section, the analytical approaches for singular particular solutions are *different*. Based on the general particular solutions (3.2) and (3.3) satisfying the Cauchy–Navier equations (2.14) and (2.15), in Section 3, for the corners with $|\theta| \le \Theta \le \pi$, first we obtain the particular solutions satisfying the boundary conditions at $\theta = \pm\Theta$, and then select the final particular solutions satisfying the boundary conditions at $\theta = 0$. In this section, the orders to satisfy the boundary conditions are switched. The boundary conditions at $\theta = 0$ are first required, and those at $\theta = \Theta$ are then added into. In both approaches, the separation techniques in dealing with the complicated boundary conditions are developed to greatly simplify the derivation for singular properties and particular solutions at corners of linear elastostatics, which are derived by calculus. Hence, one of the contributions of this paper is such an effective systematic analysis, which enriches both the theory of linear elastostatics and its numerical methods.

## 6. Model B of crack singularity and its numerical solutions

### 6.1. Model B of crack singularity

In this section, let us consider the interior crack of symmetric models with free stress for (5.1) and (5.6) at $\Theta = \pi$:

$$v = u_y = 0 \quad \text{at } \theta = 0, \tag{6.1}$$

$$\sigma_{xy} = 0, \quad \sigma_y = 0 \ \text{ at } \theta = \pi. \tag{6.2}$$

From the boundary conditions (6.2) at $\theta = \pi$ we have

$$\sigma_{xy} = 2\mu\sum_{k=1}^{L} v_k r^{v_k-1}\{b_k[(D(v_k-1))\sin(v_k-3)\pi] + d_k\sin(v_k-1)\pi\} = 0, \tag{6.3}$$

$$\begin{aligned}\sigma_y = 2\sum_{k=1}^{L} v_k r^{v_k-1}\{&b_k[(\lambda+\mu)(1-D)\cos(v_k-1)\pi \\ &+ \mu D(v_k-1)\cos(v_k-3)\pi] + d_k[\mu\cos(v_k-1)\pi]\} = 0.\end{aligned} \tag{6.4}$$

Based on Theorem 5.1, when $\Theta = \pi$, we also conclude that $v^* = n$ and $v^* = n + \frac{1}{2}$. The particular solutions are split into two cases: (1) $v^* = n + \frac{1}{2}$ and (2) $v^* = n$. First for $v^* = n + \frac{1}{2}$, from (6.3) we have the relations of coefficients

$$d_{2n+1} = -D(n-\tfrac{1}{2})b_{2n+1}, \tag{6.5}$$

and for $v^* = n$ from (6.4),

$$d_{2n} = \frac{-(\lambda+\mu)(1-D)+\mu D(1-n)}{\mu} b_{2n}. \tag{6.6}$$

Then the solutions (5.16) and (5.17) lead to

$$\begin{aligned}u_L = &\sum_{n=0}^{L-1} r^{n+1/2} b_{2n+1}\left[\left(D\left(n-\frac{1}{2}\right)+1\right)\cos\left(n+\frac{1}{2}\right)\theta\right. \\ &\left. - D\left(n+\frac{1}{2}\right)\cos\left(n-\frac{3}{2}\right)\theta\right] \\ &+ \sum_{n=1}^{L} r^n b_{2n}\left[\frac{\lambda(1-D)+2\mu(1-D)+\mu Dn}{\mu}\cos n\theta - Dn\cos(n-2)\theta\right] \\ &+ b_0,\end{aligned} \tag{6.7}$$

$$\begin{aligned}v_L = &\sum_{n=0}^{L-1} r^{n+1/2} b_{2n+1}\left[\left(D\left(-n+\frac{1}{2}\right)+1\right)\sin\left(n+\frac{1}{2}\right)\theta\right. \\ &\left. + D\left(n+\frac{1}{2}\right)\sin\left(n-\frac{3}{2}\right)\theta\right] \\ &+ \sum_{n=1}^{L} r^n b_{2n}\left[\frac{-\lambda(1-D)+2\mu D-\mu Dn}{\mu}\sin n\theta + Dn\sin(n-2)\theta\right].\end{aligned} \tag{6.8}$$

By means of (5.26), the final particular solutions are obtained:

$$u_L=\sum_{n=0}^{L-1} r^{n+1/2}\left\{b_{2n+1}\left[\left(D\left(n-\frac{1}{2}\right)+1\right)\cos\left(n+\frac{1}{2}\right)\theta -D\left(n+\frac{1}{2}\right)\cos\left(n-\frac{3}{2}\right)\theta\right]\right\}+\sum_{n=1}^{L} r^n\{b_{2n}[(D(n+1)+1)\cos n\theta -Dn\cos(n-2)\theta]\}+b_0, \tag{6.9}$$

$$v_L=\sum_{n=0}^{L-1} r^{n+1/2}\left\{b_{2n+1}\left[\left(D\left(-n+\frac{1}{2}\right)+1\right)\sin\left(n+\frac{1}{2}\right)\theta +D\left(n+\frac{1}{2}\right)\sin\left(n-\frac{3}{2}\right)\theta\right]\right\}+\sum_{n=1}^{L} r^n\{b_{2n}[(-D(n+1)+1)\sin n\theta +Dn\sin(n-2)\theta\}. \tag{6.10}$$

### 6.2. Numerical results

When the particular solutions (6.9) and (6.10) replace (4.6) and (4.7) in Model A, we obtain Model B with the following boundary conditions:

$$\sigma_{xy}=\sigma_y=0 \quad \text{on } \overline{OD}, \tag{6.11}$$

$$v=u_y=0 \quad \text{on } \overline{OA}\cup\overline{CB}, \tag{6.12}$$

$$u=v_x=0 \quad \text{on } \overline{CD}, \tag{6.13}$$

$$u=1, \quad v_x=0 \ \text{ on } \overline{AB}. \tag{6.14}$$

Since the particular solutions (6.9) and (6.10) satisfy the Cauchy–Navier equation (2.5) and the boundary conditions on $\overline{OA}\cup\overline{OD}$ already, the coefficients $b_i$ are sought by satisfying the rest boundary conditions in (6.12)–(6.14). The same CTM in Section 4.2 is also valid for Model B. The errors and condition numbers are listed in Tables 6–9, from which we can find the same rates as in (4.25) and (4.26).

## 7. Leading powers $v_k$ of the corner solutions $O(r^{v_k})$

### 7.1. Algorithms

In this section, we study the leading $v_k=\alpha_k+i\beta_k$ for the corner solutions, where $\alpha_k,\beta_k\in\Re$. Consider (3.13) as an example, since Eq. (5.29) is a special case at $D=1$ with sign " $-$" . For complex roots of $v^*=\alpha+i\beta$, we convert (3.13) to two real equations of $\alpha$ and $\beta$ as follows.

Since

$$\sin\mathbf{z}=\frac{e^{iz}-e^{-iz}}{2i}, \tag{7.1}$$

we obtain from (3.13)

$$\frac{e^{i2(\alpha+i\beta)\Theta}-e^{-i2(\alpha+i\beta)\Theta}}{2i}=\pm D(\alpha+i\beta)\sin 2\Theta. \tag{7.2}$$

For the real part of (7.2) we have

$$\frac{e^{-2\beta\Theta}+e^{2\beta\Theta}}{2}\sin 2\alpha\Theta=\pm D\alpha\sin 2\Theta, \tag{7.3}$$

to give

$$\cosh(2\beta\Theta)\sin 2\alpha\Theta=\pm D\alpha\sin 2\Theta. \tag{7.4}$$

For the imaginary part of (7.2), we have

$$\frac{e^{2\beta\Theta}-e^{-2\beta\Theta}}{2}\cos 2\alpha\Theta=\pm D\beta\sin 2\Theta,$$

to give

$$\sinh(2\beta\Theta)\cos 2\alpha\Theta=\pm D\beta\sin 2\Theta. \tag{7.5}$$

Then we may apply the Newton iteration, to seek two real $\alpha$ and $\beta$ by satisfying (7.4) and (7.5).

**Table 6**
Errors, condition numbers and the leading coefficients $b_1$ and $b_0$ for Model B by the CTM as $D=\frac{1}{2}$.

| $M$ | $L$ | $\|\varepsilon\|_B$ | $\|\delta(u)\|_{\infty,\overline{AB}\cup\overline{CD}}$ | $\|\delta(v)\|_{\infty,\overline{BC}}$ | Cond | Cond_eff | $b_1$ | $b_0$ |
|---|---|---|---|---|---|---|---|---|
| 3 | 4 | 6.42(−3) | 5.71(−3) | 4.92(−3) | 1.88(1) | 2.37 | 0.190614727092869 | 0.460409333521642 |
| 6 | 8 | 2.60(−4) | 2.19(−4) | 2.36(−4) | 1.68(2) | 3.92 | 0.191436302772700 | 0.460488642952438 |
| 9 | 12 | 2.67(−5) | 2.77(−5) | 2.40(−5) | 1.24(3) | 5.95 | 0.191431830741538 | 0.460491701207298 |
| 12 | 16 | 2.51(−6) | 2.71(−6) | 2.23(−6) | 7.92(3) | 8.23 | 0.191430875888065 | 0.460492795062574 |
| 15 | 20 | 2.58(−7) | 2.96(−7) | 2.37(−7) | 4.61(4) | 10.7 | 0.191430793209968 | 0.460492860222083 |
| 18 | 24 | 2.69(−8) | 3.29(−8) | 2.64(−8) | 2.50(5) | 13.2 | 0.191430788743211 | 0.460492862324388 |
| 21 | 28 | 2.85(−9) | 3.69(−9) | 3.01(−9) | 1.30(6) | 15.8 | 0.191430788341483 | 0.460492862332309 |
| 24 | 32 | 3.02(−10) | 4.16(−10) | 3.44(−10) | 6.47(6) | 18.5 | 0.191430788360548 | 0.460492862295949 |
| 27 | 36 | 3.21(−11) | 4.70(−11) | 3.92(−11) | 3.14(7) | 21.1 | 0.191430788363848 | 0.460492862291750 |
| 30 | 40 | 3.43(−12) | 5.34(−12) | 4.46(−12) | 1.49(8) | 23.8 | 0.191430788364732 | 0.460492862291075 |

**Table 7**
Errors, condition numbers and the leading coefficients $b_1$ and $b_0$ for Model B by the CTM as $D=\frac{5}{11}$.

| $M$ | $L$ | $\|\varepsilon\|_B$ | $\|\delta(u)\|_{\infty,\overline{AB}\cup\overline{CD}}$ | $\|\delta(v)\|_{\infty,\overline{BC}}$ | Cond | Cond_eff | $b_1$ | $b_0$ |
|---|---|---|---|---|---|---|---|---|
| 3 | 4 | 4.57(−3) | 4.07(−3) | 3.66(−3) | 1.78(1) | 2.46 | 0.142950891214175 | 0.464934155574646 |
| 6 | 8 | 1.82(−4) | 1.50(−4) | 1.67(−4) | 1.57(2) | 4.06 | 0.143640461098265 | 0.464855368553578 |
| 9 | 12 | 1.86(−5) | 1.93(−5) | 1.72(−5) | 1.16(3) | 6.15 | 0.143639690785542 | 0.464854952373997 |
| 12 | 16 | 1.74(−6) | 1.89(−6) | 1.60(−6) | 7.36(3) | 8.47 | 0.143638839420185 | 0.464855849789067 |
| 15 | 20 | 1.78(−7) | 2.08(−7) | 1.70(−7) | 4.27(4) | 11.0 | 0.143638760656728 | 0.464855919706794 |
| 18 | 24 | 1.86(−8) | 2.31(−8) | 1.89(−8) | 2.33(5) | 13.6 | 0.143638755600059 | 0.464855923599455 |
| 21 | 28 | 1.96(−9) | 2.60(−9) | 2.16(−9) | 1.20(6) | 16.3 | 0.143638755231839 | 0.464855923749553 |
| 24 | 32 | 2.08(−10) | 2.94(−10) | 2.47(−10) | 6.02(6) | 19.0 | 0.143638755246206 | 0.464855923724844 |
| 27 | 36 | 2.21(−11) | 3.33(−11) | 2.82(−11) | 2.92(7) | 21.8 | 0.143638755249903 | 0.464855923720447 |
| 30 | 40 | 2.36(−12) | 3.79(−12) | 3.22(−12) | 1.39(8) | 24.6 | 0.143638755250735 | 0.464855923719710 |

Please cite this article as: Li Z-C, et al. Models of corner and crack singularity of linear elastostatics and their numerical solutions. Eng Anal Bound Elem (2010), doi:10.1016/j.enganabound.2010.01.001

### 7.2. Numerical results for $\Theta = \pi/4, 3\pi/4$

The constants $D = \frac{1}{2}$ and $\frac{5}{11}$ correspond to the corners under the clamped boundary conditions, and $D = 1$ to those under free stress boundary conditions. We only investigate two cases numerically: (1) $\Theta = \pi/4$ and (2) $\Theta = 3\pi/4$, which correspond to the rectangular corners and the concave corners of L-shaped domains, respectively. Note that such two cases are often used in engineering applications.

First $\Theta = \pi/4$, the leading $v_k$ are listed in Tables 10–12 for $D = \frac{1}{2}, \frac{5}{11}, 1$, respectively, where "*symmetric*" and "*anti-symmetric*" denote the symmetric and the anti-symmetric models of crack singularity, respectively. The minimal $v_1$ is real, to have

$$v_1 = \alpha_1 = 1.473 \quad \text{for } D = \tfrac{1}{2}, \tag{7.6}$$

$$v_1 = \alpha_1 = 1.516 \quad \text{for } D = \tfrac{5}{11}, \tag{7.7}$$

$$v_1 = \alpha_1 = 1 \quad \text{for } D = 1. \tag{7.8}$$

From (7.6) and (7.7), although the derivatives of solutions $u$ and $v$ at the rectangular angles are bounded for the clamped boundary conditions, the second order derivatives are unbounded. Since for $u = O(r^p)$, where $p(>1)$ is noninteger, $u \in H^{p+1-\delta}(S)$, $0 < \delta \ll 1$. We conclude that $u, v \in H^2(S)$ but not in $H^3(S)$. This implies that for the corners with clamped boundary conditions, the linear elements may retain the optimal convergence rates $O(h)$ in $H^1$ norm (see [2]), where $h$ is the maximal boundary length of quasi-unform triangular elements. However, high order elements will lead to reduced convergence rates. For the rectangular corners with free stress boundary conditions, since $v_2 = 2.739 \pm 1.119i$ with the solution

$$u = O(|r^{v_2}|) = O(r^{\alpha_2}) = O(r^{2.739}), \tag{7.9}$$

the solutions $u, v \in H^3(S)$ but not in $H^4(S)$. The quadratic elements retain the optimal convergence rates $O(h^2)$ in $H^1$ norm, but the cubic elements will lead to reduction of convergence rates.

For the L-shaped domains, the leading $v_k$ are listed in Tables 13–15. We can see that the minimal $v_1$ are also real, with

$$v_1 = \alpha_1 = 0.6018 \quad \text{for } D = \tfrac{1}{2}, \tag{7.10}$$

$$v_1 = \alpha_1 = 0.6073 \quad \text{for } D = \tfrac{5}{11}, \tag{7.11}$$

$$v_1 = \alpha_1 = 0.5445 \quad \text{for } D = 1. \tag{7.12}$$

For $\Theta = 3\pi/4$ and $\Theta = \pi$, all elements including linear elements suffer from reduction of convergence rates. Special treatments, such as local refinements or some combining techniques, must be done to recover the optimal convergence rates. Note that the leading $v_k$ in Table 15 for symmetric Model B are consistent with those in [28].

**Table 8**
The leading coefficients for Model B by the CTM as $D = \frac{1}{2}$ and $L = 40$, where "Sig." denotes the number of significant digits.

| $i$ | All digits | Sig. | $i$ | All digits | Sig. |
|---|---|---|---|---|---|
| 0 | **4.60492862291**075(−1) | 12 | 41 | −**1.73**245721041029(−9) | 3 |
| 1 | **1.91430788364**732(−1) | 12 | 42 | −**1.0395**6126266378(−8) | 5 |
| 2 | **2.85280692235**259(−1) | 11 | 43 | **1.206**85830625993(−8) | 4 |
| 3 | **8.65384735**258162(−2) | 10 | 44 | −**5.79**1010411447 17(−9) | 3 |
| 4 | −**2.55693135**993185(−2) | 10 | 45 | **3.3**1772120246795(−10) | 2 |
| 5 | **1.12833957**531029(−2) | 10 | 46 | **2.503**96655966956(−9) | 4 |
| 6 | **1.91331418**311528(−3) | 10 | 47 | −**2.6**3458948729947(−9) | 2 |
| 7 | −**7.29750804**546592(−3) | 9 | 48 | **1.3**7788599118725(−9) | 2 |
| 8 | **5.63263716**152084(−3) | 11 | 49 | −**7.**81162737992002(−11) | 1 |
| 9 | −**2.35009479**678666(−3) | 10 | 50 | −**6.0**3279317962677(−10) | 2 |
| 10 | −**9.80803172**348266(−4) | 11 | 51 | **6.8**1931704576686(−10) | 2 |
| 11 | **1.96266629**467748(−3) | 10 | 52 | −**3.2**8515036709205(−10) | 2 |
| 12 | −**7.46651498**965064(−4) | 10 | 53 | **1.5**5739979004667(−11) | 2 |
| 13 | **6.23424546**041238(−5) | 8 | 54 | **1.4**5343899357852(−10) | 2 |
| 14 | **2.65521468**684286(−4) | 10 | 55 | −**1.5**0932163298223(−10) | 2 |
| 15 | −**2.77056393**891716(−4) | 9 | 56 | **7.**77541520065562(−11) | 1 |
| 16 | **1.51628454**593015(−4) | 9 | 57 | −3.13825577609254(−12) | 0 |
| 17 | −**2.19532639**405031(−5) | 8 | 58 | −**3.4**9090836910167(−11) | 2 |
| 18 | −**5.63865516**422603(−5) | 9 | 59 | **3.**81299801519005(−11) | 1 |
| 19 | **8.01093895**492351(−5) | 7 | 60 | −**1.**80595862796830(−11) | 1 |
| 20 | −**3.79322566**760060(−5) | 8 | 61 | 5.14543788238336(−13) | 0 |
| 21 | **5.71079059**991865(−6) | 7 | 62 | 8.14500297893374(−12) | 0 |
| 22 | **1.28748497**314507(−5) | 8 | 63 | −8.14981179616867(−12) | 0 |
| 23 | −**1.52419632**807077(−5) | 7 | 64 | 4.01633148267675(−12) | 0 |
| 24 | **8.60060990**992634(−6) | 7 | 65 | −7.88269192623829(−16) | 0 |
| 25 | −**1.15292496**205150(−6) | 7 | 66 | −**1.**87087975129455(−12) | 1 |
| 26 | −**3.17347419**700668(−6) | 10 | 67 | **1.**87619156640006(−12) | 1 |
| 27 | **4.08474089**334245(−6) | 8 | 68 | −8.09085848892250(−13) | 0 |
| 28 | −**1.90803089**322337(−6) | 7 | 69 | −2.23213396539257(−14) | 0 |
| 29 | **1.57263**593698569(−7) | 6 | 70 | 3.65055237624289(−13) | 0 |
| 30 | **7.6597**4574515494(−7) | 5 | 71 | −3.22862986722333(−13) | 0 |
| 31 | −**8.2549**3465402272(−7) | 5 | 72 | 1.42466073970884(−13) | 0 |
| 32 | **4.4067**8358491772(−7) | 5 | 73 | 1.01974866208093(−14) | 0 |
| 33 | −**3.7508**6774588730(−8) | 5 | 74 | −6.70935839889025(−14) | 0 |
| 34 | −**1.81333**085487258(−7) | 6 | 75 | 5.65566193806084(−14) | 0 |
| 35 | **2.17820**940924056(−7) | 6 | 76 | −1.81107706179081(−14) | 0 |
| 36 | −**1.0380**3895641095(−7) | 5 | 77 | −3.75286265719837(−15) | 0 |
| 37 | **7.4**5466031490200(−9) | 2 | 78 | 7.41273630237582(−15) | 0 |
| 38 | **4.3235**3708053661(−8) | 5 | 79 | −3.58842381320799(−15) | 0 |
| 39 | −**4.621**62108936192(−8) | 4 | 80 | 9.27951452130156(−16) | 0 |
| 40 | **2.44**731997561589(−8) | 3 | | | |

Please cite this article as: Li Z-C, et al. Models of corner and crack singularity of linear elastostatics and their numerical solutions. Eng Anal Bound Elem (2010), doi:10.1016/j.enganabound.2010.01.001

**Table 9**
The leading coefficients for Model B by the CTM as $D=\frac{5}{11}$ and $L=40$, where "Sig." denotes the number of significant digits.

| $i$ | All digits | Sig. | $i$ | All digits | Sig. |
|---|---|---|---|---|---|
| 0 | **4.64855923719**710(−1) | 12 | 41 | −**1.30**002358332516(−9) | 3 |
| 1 | **1.43638755250**735(−1) | 12 | 42 | −**7.80**024521628120(−9) | 3 |
| 2 | **3.03295087132**863(−1) | 12 | 43 | **9.05**561197065626(−9) | 3 |
| 3 | **6.49335392949**688(−2) | 11 | 44 | −**4.34**532621085886(−9) | 3 |
| 4 | −**1.91857559037**167(−2) | 11 | 45 | **2.4**9039737143173(−10) | 2 |
| 5 | **8.46641720**917033(−3) | 9 | 46 | **1.878**78617629899(−9) | 4 |
| 6 | **1.43564193625**392(−3) | 11 | 47 | −**1.97**688238644581(−9) | 3 |
| 7 | −**5.47563420**198196(−3) | 10 | 48 | **1.0**3398435114461(−9) | 2 |
| 8 | **4.22640996033**476(−3) | 11 | 49 | −**5**.87106516868838(−11) | 1 |
| 9 | −**1.76337721**959811(−3) | 9 | 50 | −**4.52**631858602659(−10) | 3 |
| 10 | −**7.35938811228**234(−4) | 11 | 51 | **5.1**1713910025082(−10) | 2 |
| 11 | **1.47267294**852949(−3) | 9 | 52 | −**2.4**6564132014254(−10) | 2 |
| 12 | −**5.60244738**237451(−4) | 9 | 53 | **1.1**7540988491699(−11) | 2 |
| 13 | **4.677822**54609653(−5) | 7 | 54 | **1.0**9023964290564(−10) | 2 |
| 14 | **1.99232179**842158(−4) | 9 | 55 | −**1.1**3265156883767(−10) | 2 |
| 15 | −**2.0788733**0416082(−4) | 8 | 56 | **5**.83914115927364(−11) | 1 |
| 16 | **1.137733520**48571(−4) | 10 | 57 | −2.40594358473458(−12) | 0 |
| 17 | −**1.6472478**2954602(−5) | 8 | 58 | −**2**.61736992838217(−11) | 1 |
| 18 | −**4.2309255**2606481(−5) | 8 | 59 | **2**.86235616588793(−11) | 1 |
| 19 | **6.0109521**0297653(−5) | 8 | 60 | −**1.3**5788066528575(−11) | 2 |
| 20 | −**2.8462203**9174530(−5) | 8 | 61 | 4.13104658171134(−13) | 0 |
| 21 | **4.285051**85133372(−6) | 7 | 62 | **6**.09830278612258(−12) | 1 |
| 22 | **9.6605535**9429563(−6) | 8 | 63 | −6.11668697452900(−12) | 0 |
| 23 | −**1.1436700**7152096(−5) | 8 | 64 | **3**.02509031313060(−12) | 1 |
| 24 | **6.4534075**8472969(−6) | 8 | 65 | −1.32443359150393(−14) | 0 |
| 25 | −**8.65089**197798438(−7) | 6 | 66 | −1.39837111738702(−12) | 0 |
| 26 | −**2.3811941**9193964(−6) | 8 | 67 | 1.41027115971752(−12) | 0 |
| 27 | **3.06495680**608180(−6) | 9 | 68 | −6.13064061194651(−13) | 0 |
| 28 | −**1.4316776**8260352(−6) | 8 | 69 | −1.11729332319077(−14) | 0 |
| 29 | **1.18001**670760093(−7) | 6 | 70 | 2.71166432489572(−13) | 0 |
| 30 | **5.74743**668086085(−7) | 6 | 71 | −2.41842917037684(−13) | 0 |
| 31 | −**6.1940**3281960835(−7) | 5 | 72 | 1.07820342879944(−13) | 0 |
| 32 | **3.3065**9962826024(−7) | 5 | 73 | 6.48150279384403(−15) | 0 |
| 33 | −**2.814**44064384515(−8) | 4 | 74 | −4.98000339377940(−14) | 0 |
| 34 | −**1.36061**997176876(−7) | 6 | 75 | 4.26088897852638(−14) | 0 |
| 35 | **1.6344**0437469177(−7) | 5 | 76 | −1.40870342539560(−14) | 0 |
| 36 | −**7.7888**5864530271(−8) | 5 | 77 | −2.35170407080490(−15) | 0 |
| 37 | **5.593**62926520973(−9) | 4 | 78 | 5.32672726035767(−15) | 0 |
| 38 | **3.24413**255803418(−8) | 6 | 79 | −2.60872187906031(−15) | 0 |
| 39 | −**3.467**80544648267(−8) | 4 | 80 | 6.78726134655898(−16) | 0 |
| 40 | **1.836**33857165517(−8) | 4 | | | |

**Table 10**
The leading powers $v_k=\alpha_k+i\beta_k$ for $\Theta=\pi/4$ as $D=\frac{1}{2}$.

| $k$ | $\lvert v_k\rvert$ | $\alpha_k$ | $\pm\beta_k$ | Notes |
|---|---|---|---|---|
| 1 | 1.472968896483033 | 1.472968896483033 | 0 | Symmetric |
| 2 | 2.883590172061964 | 2.821716472135599 | 0.5941451264556297 | Anti-symmetric |
| 3 | 4.960770646814888 | 4.860030994229132 | 0.9946578031827807 | Symmetric |
| 4 | 6.991301093667654 | 6.883058973276537 | 1.225475480258939 | Anti-symmetric |
| 5 | 9.006921531098730 | 8.898754211636639 | 1.391692835452230 | Symmetric |
| 6 | 11.01596796529159 | 10.91026771875466 | 1.522369376147110 | Anti-symmetric |

**Table 11**
The leading powers $v_k=\alpha_k+i\beta_k$ for $\Theta=\pi/4$ as $D=\frac{5}{11}$.

| $k$ | $\lvert v_k\rvert$ | $\alpha_k$ | $\pm\beta_k$ | Notes |
|---|---|---|---|---|
| 1 | 1.516014376393271 | 1.516014376393271 | 0 | Symmetric |
| 2 | 2.876843140370182 | 2.831918346035538 | 0.5064236721188217 | Anti-symmetric |
| 3 | 4.954286448691338 | 4.866771089072888 | 0.9270886593260231 | Symmetric |
| 4 | 6.985315586102505 | 6.888090199255578 | 1.161398830878450 | Anti-symmetric |
| 5 | 9.001406678875039 | 8.902765006809342 | 1.328945985368559 | Symmetric |

Please cite this article as: Li Z-C, et al. Models of corner and crack singularity of linear elastostatics and their numerical solutions. Eng Anal Bound Elem (2010), doi:10.1016/j.enganabound.2010.01.001

**Table 12**
The leading powers $v_k=\alpha_k+i\beta_k$ for $\Theta=\pi/4$ as $D=1$.

| $k$ | $\lvert v_k\rvert$ | $\alpha_k$ | $\pm\beta_k$ | Notes |
|---|---|---|---|---|
| 1 | 1.000000000000000 | 1.000000000000000 | 0 | Anti-symmetric |
| 2 | 2.959322163347230 | 2.739593356324596 | 1.119024534342417 | Symmetric |
| 3 | 5.026167618453784 | 4.808250761274224 | 1.463928121698337 | Anti-symmetric |
| 4 | 7.048671547685778 | 6.845135158415644 | 1.681634695817452 | Symmetric |
| 5 | 9.058170509436751 | 8.868825977288248 | 1.842383988914041 | Anti-symmetric |

**Table 13**
The leading powers $v_k=\alpha_k+i\beta_k$ for $\Theta=3\pi/4$ as $D=\frac{1}{2}$.

| $k$ | $\lvert v_k\rvert$ | $\alpha_k$ | $\pm\beta_k$ | Notes |
|---|---|---|---|---|
| 1 | 0.6018077748921469 | 0.6018077748921469 | 0 | Anti-symmetric |
| 2 | 0.7480105399586175 | 0.7480105399586175 | 0 | Symmetric |
| 3 | 1.197155208081384 | 1.197155208081384 | 0 | Symmetric |
| 4 | 1.515859334469746 | 1.515859334469746 | 0 | Anti-symmetric |
| 5 | 1.769542924220030 | 1.769542924220030 | 0 | Anti-symmetric |
| 6 | 2.314991817379920 | 2.311922516085420 | 0.1191696024716203 | Symmetric |
| 7 | 2.987516960464614 | 2.980572754944220 | 0.2035771144995205 | Anti-symmetric |
| 8 | 3.657905678935235 | 3.648833242301695 | 0.2574683006910641 | Symmetric |
| 9 | 4.327132525489046 | 4.316814106856850 | 0.2986500627605933 | Anti-symmetric |
| 10 | 4.995656188906412 | 4.984586568184292 | 0.3323815609140698 | Symmetric |
| 11 | 5.663722020440595 | 5.652198969558337 | 0.3611010015873168 | Anti-symmetric |
| 12 | 6.331473472644984 | 6.319685412164409 | 0.3861769362397296 | Symmetric |
| 13 | 6.999000115449453 | 6.987070716017204 | 0.4084671656771136 | Anti-symmetric |
| 14 | 7.666360777162631 | 7.654373422385060 | 0.4285499694351287 | Symmetric |
| 15 | 8.333595680316281 | 8.321607690233166 | 0.4468360021735137 | Anti-symmetric |
| 16 | 9.000733241572054 | 8.988784537764895 | 0.4636285361999712 | Symmetric |
| 17 | 9.667794090581419 | 9.655912680380271 | 0.4791585194405920 | Anti-symmetric |

**Table 14**
The leading powers $v_k=\alpha_k+i\beta_k$ for $\Theta=3\pi/4$ as $D=\frac{5}{11}$.

| $k$ | $\lvert v_k\rvert$ | $\alpha_k$ | $\pm\beta_k$ | Notes |
|---|---|---|---|---|
| 1 | 0.6073157318928521 | 0.6073157318928521 | 0 | Anti-symmetric |
| 2 | 0.7394036691720525 | 0.7394036691720525 | 0 | Symmetric |
| 3 | 1.209777500433687 | 1.209777500433687 | 0 | Symmetric |
| 4 | 1.491410518278246 | 1.491410518278246 | 0 | Anti-symmetric |
| 5 | 1.797134735821410 | 1.797134735821410 | 0 | Anti-symmetric |
| 6 | 2.314293111851054 | 2.313209321200484 | 0.07081838654211584 | Symmetric |
| 7 | 2.986799444886649 | 2.981659858658838 | 0.1751439728844643 | Anti-symmetric |
| 8 | 3.657186684714524 | 3.649772911248499 | 0.2327490991816481 | Symmetric |
| 9 | 4.326421108148834 | 4.317640684137880 | 0.2754968742348289 | Anti-symmetric |
| 10 | 4.994957136285802 | 4.985323780447036 | 0.3100703104809264 | Symmetric |
| 11 | 5.663037791558908 | 5.652863867215116 | 0.3393038864471669 | Anti-symmetric |
| 12 | 6.330805206958780 | 6.320290643545786 | 0.3647200975597538 | Symmetric |
| 13 | 6.998348187195060 | 6.987625912969009 | 0.3872485630966425 | Anti-symmetric |
| 14 | 7.665725112460134 | 7.654886082677711 | 0.4075052895718210 | Symmetric |
| 15 | 8.332975944262848 | 8.322083760631754 | 0.4259224914142927 | Anti-symmetric |
| 16 | 9.000128951202512 | 8.989228811532170 | 0.4428165672076442 | Symmetric |
| 17 | 9.667204684174683 | 9.656329075638490 | 0.4584268629864869 | Anti-symmetric |

The fundamental solutions also satisfy the Cauchy–Navier equation (see [13,40]). However, since they are smooth functions, poor solutions near the concave corners are obtained. For the corners with the clamped and free stress boundary conditions, we may solicit the combined algorithms in [19,20] to choose both fundamental solutions and the leading particular solutions (3.24) and (3.25) with $v_k$ given in Tables 10, 11, 13 and 14.

## 8. Concluding remarks

To close this paper, let us address the novelties in this paper.

1. The singularity properties are explored for linear elastostatics at corners with the clamped and the free stress boundary conditions. The singularity properties for corner with *the clamped boundary conditions* in this paper are new, compared with the existing literature, such as Williams [38], Lin and Tong [28], Jirousek and Venkstesh [14], Jirousek and Wroblewski [15], Piltner [32], Domingues et al. [6], and Qin [36], where only the free traction conditions of corners are discussed. There also exists lack for a systematic analysis on the singularity properties and particular solutions of linear elastostatics, although many papers have cited and used them. This paper is also devoted to develop such a systematic analysis. By the separation techniques, the singularity properties and particular solutions satisfying the

Please cite this article as: Li Z-C, et al. Models of corner and crack singularity of linear elastostatics and their numerical solutions. Eng Anal Bound Elem (2010), doi:10.1016/j.enganabound.2010.01.001

**Table 15**
The leading powers $v_k=\alpha_k+i\beta_k$ for $\Theta=3\pi/4$ as $D=1$.

| $k$ | $\lvert v_k\rvert$ | $\alpha_k$ | $\pm\beta_k$ | Notes |
|---|---|---|---|---|
| 1 | 0.5444837367824639 | 0.5444837367824639 | 0 | Symmetric |
| 2 | 0.9085291898460988 | 0.9085291898460988 | 0 | Anti-symmetric |
| 3 | 1 | 1 | 0 | Anti-symmetric |
| 4 | 1.645586951597062 | 1.629257376759570 | 0.2312505471151075 | Symmetric |
| 5 | 2.322898854922502 | 2.301327060714402 | 0.3158367455250936 | Anti-symmetric |
| 6 | 2.995276274143960 | 2.971843773159274 | 0.3739312054164139 | Symmetric |
| 7 | 3.665422571806732 | 3.641420097721594 | 0.4187867020567064 | Anti-symmetric |
| 8 | 4.334377325063357 | 4.310377291541205 | 0.4554935790867853 | Symmetric |
| 9 | 5.002626455466441 | 4.978902198949798 | 0.4866254681226541 | Anti-symmetric |
| 10 | 5.670427007109263 | 5.647111773660799 | 0.5136838120241800 | Symmetric |
| 11 | 6.337927206429769 | 6.315083377631776 | 0.5376273872874201 | Anti-symmetric |
| 12 | 7.005218173009443 | 6.982870441506594 | 0.5591082619629875 | Symmetric |
| 13 | 7.672358758411265 | 7.650511172997483 | 0.5785911420085266 | Anti-symmetric |
| 14 | 8.339388500645805 | 8.318033687816522 | 0.5964194271257102 | Symmetric |
| 15 | 9.006334830959638 | 8.985459178447304 | 0.6128543381700597 | Anti-symmetric |
| 16 | 9.673217297603455 | 9.652803949157894 | 0.6280993597962390 | Symmetric |

complicated boundary conditions can be derived by calculus. See Remark 5.2.

2. The explicit singular solutions with respect to the displacements $u$ and $v$ are first found for the interior crack (i.e., the crack tip with $\Theta=\pi$). For the free traction boundary conditions of the crack tip, the explicit complex solutions were also provided by Piltner [32] (also see [6]). Since $z=u+iv$, the explicit complex solutions are equivalent to the explicit solutions in Sections 5 and 6. However, since the solutions of $u$ and $v$ satisfying the Cauchy–Navier equations (2.14) and (2.15) are simpler than the complex solutions in [32], the explicit singular solutions of the crack tip in this paper may find wider applications.
3. Two crack models (called Models A and B) are designed, and their highly accurate solutions are obtained by the collocation Trefftz method (CTM). The leading coefficient reaches 12–14 significant digits by the computation in double precision. Those accurate solutions can be used, to examine other numerical solutions for singularity problems as in [19].
4. The singular solutions for linear elastostatics at corners are *essential* in both theory and computation. The algorithms to seek the leading powers $v_k=\alpha_k+i\beta_k$ of the corner solution $O(r^{v_k})$ are given in Section 7, and in particular, the value of $v_k$ for $\Theta=\pi/4$ and $\Theta=3\pi/4$, are provided numerically. Those powers are important for the finite element analysis, and for designing new numerical algorithms. Note that the interior crack, the rectangular corner and the concave corner of the L-shaped domain are most often used in engineering.
5. The analysis of corner singularity in this paper is made directly from the Cauchy–Navier equation (2.5), and it is different from the biharmonic equations at corner for the free stress boundary conditions in Williams [38]. Both the approaches and the results in this paper are significant for linear elastostatics with singularity.
6. Since the linear elastostatics is more complicated than Poisson's, biharmonic and Helmholtz equations, the analysis and results of this paper may greatly enrich both the linear elastostatics theory and its numerical methods, such as the combined method [19] and the Trefftz methods, which include the boundary approximation method [26,18], the collocation Trefftz method [24,3], the hybrid Trefftz method [10,11,14,15,36], the boundary collocation techniques [16], the Trefftz-FEM [5,37], the dual method [33], etc.

## Acknowledgements

We are grateful for reviewers for their valuable comments and suggestions, and we are also indebted to H.C. Hsieh for some numerical computation in Section 7.

## References

[1] Akella MR, Kotamraju GR. Trefftz indirect method applied to nonlinear potential problems. Eng Anal Bound Elem 2000;24:459–65.
[2] Brenner SC, Scott LR. The mathematical theory of finite element methods. New York: Springer; 1994.
[3] Chen JT, Lee YT, Shieh SC. Revisit of two classical elasticity problems by using the Trefftz method. Eng Anal Bound Elem 2009;33:890–5.
[4] Chen YW, Liu CS, Chang JR. Applications of the modified Trefftz method for the Laplace equation. Eng Anal Bound Elem 2009;33:137–46.
[5] Cui YH, Wang J, Dhanasekar M, Qin QH. Model III fracture analysis by Trefftz boundary element method. Acta Mech Sin 2007;23:173–81.
[6] Domingues JS, Portela A, de Castro PMST. Trefttz boundary element method applied to fracture mechanics. Eng Fract Mech 1999;64:67–86.
[7] Dong CY, Lo SH, Cheung YK, Lee KY. Anisotropic thin plate bending problems by Trefftz boundary collocation method. Eng Anal Bound Elem 2004;28:1017–24.
[8] Drombosky TW, Meyer AL, Ling L. Applicability of the method of fundamental solutions. Eng Anal Bound Elem 2009;33:637–43.
[9] Elliotis M, Georgiou G, Xenophontos C. The singular function boundary integral method for biharmonic problems with crack singularities. Eng Anal Bound Elem 2007;31:209–15.
[10] de Freitas JAT, Ji ZY. Hybrid-Trefftz finite element formulation for simulation of singular stress fields. Int J Numer Methods Eng 1996;39:281–308.
[11] de Freitas JAT, Ji ZY. Hybrid-Trefftz equilibrium model for crack problems. Int J Numer Methods Eng 1996;39:569–84.
[12] Guimaraes S, Telles JCF. The method of fundamental solutions for fracture mechanics—Reissner's plate application. Eng Anal Bound Elem 2009;33:1152–60.
[13] Hsiao GC, Wendland WL. Boundary integral equations. Berlin: Springer; 2008.
[14] Jirousek J, Venkstesh A. Hybrid Trefftz plane elasticity element with p-method capabilities. Int J Numer Eng 1992;35:1443–72.
[15] Jirousek J, Wroblewski A. T-element: state of the art and future trends. Arch Comput Methods Eng 1996;3:323–434.
[16] Kolodziej JA, Zielinski AP. Boundary collocation techniques and their application in engineering. Southampton, Boston: WIT Press; 2009.
[17] Leitao VMA. Applications of multi-region Trefftz-collocation to fracture mechanics. Eng Anal Bound Elem 1998;22:251–6.
[18] Li ZC. Numerical methods for Elliptic problems with singularities: boundary methods and nonconforming combinations. Singapore: World Scientific; 1990.
[19] Li ZC. Combined methods for Elliptic equations with singularities, interfaces and infinities. Boston: Kluwer Academic Publishers; 1998.
[20] Li ZC. Combinations of method of fundamental solutions for Laplace's equation with singularities. Eng Anal Bound Elem 2008;32:856–69.
[21] Li ZC, Chien CS, Huang HT. Effective condition number for finite difference method. J Comput Appl Math 2007;198:208–35.
[22] Li ZC, Huang TH. Study on effective condition number for collocation methods. Eng Anal Bound Elem 2008;32:839–48.

Please cite this article as: Li Z-C, et al. Models of corner and crack singularity of linear elastostatics and their numerical solutions. Eng Anal Bound Elem (2010), doi:10.1016/j.enganabound.2010.01.001

[23] Li ZC, Lu TT, Hu HY. The collocation Trefftz method for biharmonic equations with crack singularities. Eng Anal Bound Elem 2004;28:79–96.
[24] Li ZC, Lu TT, Hu HY, Cheng AHD. Trefftz and collocation methods. Southampton, Boston: WIT Press; 2008.
[25] Li ZC, Lu TT, Wei Y. Effective condition number of Trefftz methods for biharmonic equations with crack singularities. Numer Linear Algebra Appl 2009;18:145–71.
[26] Li ZC, Mathon R, Sermer P. Boundary methods for solving elliptic problems with singularities and interfaces. SIAM J Numer Anal 1987;24:487–98.
[27] Liu CS. An effectively modified direct Trefftz method for 2D potential problems considering the domain's characteristic length. Eng Anal Bound Elem 2007;31:983–93.
[28] Lin KY, Tong P. Singular finite element for the fracture analysis of V-notched plate. Int J Numer Methods Eng 1980;15:1343–54.
[29] Liu X, Wu X. Differential quadrature Trefftz method for irregular plate problems. Eng Anal Bound Elem 2009;33:363–7.
[30] Lu TT, Chang CM, Huang HT, Li ZC. Stability analysis of Trefftz methods for the stick–slip problem. Eng Anal Bound Elem 2009;33:474–84.
[31] Lu TT, Hu HY, Li ZC. Highly accurate solutions of Motz's and the cracked beam problems. Eng Anal Bound Elem 2004;28:1387–403.
[32] Piltner R. Recent developments in Trefftz method for finite element and boundary applications. Adv Eng Software 1995;24:107–15.
[33] Portela A, Alliabadi MH, Rooke DP. The dual boundary element method: effective implementation for crack problems. Int J Numer Methods Eng 1992;33:1269–87.
[34] Portela A, Charafi A. Trefftz boundary element method for domains with slits. Eng Anal Bound Elem 1997;20:299–304.
[35] Shaw RP, Huang SC, Zhao CX. The embedding integral and the Trefftz method for potential problems with partitioning. Eng Anal Bound Elem 1992;9:83–90.
[36] Qin QH. The Trefftz finite and boundary element method. Southampton, Boston: WIT Press; 2000 282pp.
[37] Wang J, Cui YH, Qin QH, Jia JY. Application of Trefftz BEM to anti-plane piezoelectric problem. Acta Mech Sin 2006;19:352–64.
[38] Williams ML. Stress singularities resulting from various boundary conditions in angular corners of plates in extension. J Appl Mech 1952;19:526–8.
[39] Wu X, Du H, Kong W. Differential quadrature Trefftz method for Poisson-type problems on irregular domains. Eng Anal Bound Elem 2008;32:413–23.
[40] Yu D. National boundary integral method and its applications. Beijing, New York: Science Press, Kluwer Academic Publishers; 2002.

Please cite this article as: Li Z-C, et al. Models of corner and crack singularity of linear elastostatics and their numerical solutions. Eng Anal Bound Elem (2010), doi:10.1016/j.enganabound.2010.01.001